NASA CR - 132731
(SER - 50944)

STUDY TO INVESTIGATE DESIGN, FABRICATION AND TEST OF LOW COST CONCEPTS FOR LARGE HYBRID COMPOSITE HELICOPTER FUSELAGE - PHASE I

by

K. M. Adams and J. J. Lucas

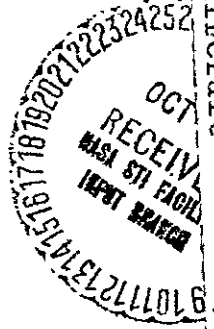

Prepared under Contract No. NASI-13479

by

Sikorsky Aircraft

Division of United Technologies Corporation,

Stratford, Conn.

June 1975

for

NATIONAL AERONAUTICS AND SPACE ADMINISTRATION

NASA CR - 132731
(SER - 50944)

STUDY TO INVESTIGATE DESIGN, FABRICATION AND TEST OF LOW COST CONCEPTS FOR LARGE HYBRID COMPOSITE HELICOPTER FUSELAGE - PHASE I

by

K. M. Adams and J. J. Lucas

Prepared under Contract No. NASI-13479

by

Sikorsky Aircraft

Division of United Technologies Corporation,

Stratford, Conn.

June 1975

for

NATIONAL AERONAUTICS AND SPACE ADMINISTRATION

THIS PAGE LEFT INTENTIONALLY BLANK

FOREWORD

This report was prepared by Sikorsky Aircraft, Division of United Technologies Corporation, under NASA contract NAS1-13479 and covers the work performed during the period August 1974 through June 1975. This report is the final Phase I report and summarizes the Phase I activity. This program was jointly funded by the Materials Division of NASA-Langley Research Center and the U.S. Army Air Mobility Research and Development Laboratory (Langley Directorate). The NASA-Langley Technical Monitor for this contract was R. L. Foye. The Sikorsky Aircraft Program Manager was J. J. Lucas.

The authors wish to acknowledge the contributions of the following Sikorsky personnel: G. Lattin and S. Svensson, Materials Engineering; D. Lowry, Structures Engineering; G. Schneider, Structural Analysis; P. Perschbacher, Test Engineering; K. Schneider, Manufacturing Engineering; and M. J. Rich, Chief Structures Technology for his overall guidance and consultation in the preparation of this report.

UNITS

Dimensional information is presented in the International System of Units (SI). The equivalent values in the U.S. customary system are shown in parentheses. All calculations were performed in the customary system and converted to the SI units. An exception is made in the Design and Analytical Section where all mathematical calculations are performed in the U.S. customary system, and in certain drawings and figures where only the U.S. customary system is utilized.

CONTENTS

LIST OF ILLUSTRATIONS

LIST OF TABLES

THIS PAGE LEFT INTENTIONALLY BLANK

STUDY TO INVESTIGATE THE DESIGN, FABRICATION, AND TEST OF LOW COST CONCEPTS FOR LARGE HYBRID COMPOSITE HELICOPTER FUSELAGE*

by

K.M. Adams and J.J. Lucas

Sikorsky Aircraft
Division of United Technologies
Stratford, Connecticut

SUMMARY

The development of a frame/stringer/skin fabrication technique for composite airframe construction promises to provide a low cost approach to the manufacturer of large helicopter airframe components. This low cost fabrication technique is dependent on the development of a single cure of the assembled composite structure, the selection of cure compatible constituent materials which comprise that structure, and the utilization of an economical and reliable tooling concept to produce the structure.

A center cabin aluminum airframe section of the Sikorsky CH-53D, a typical current production transport helicopter was selected for evaluation as a composite structure. The design, as developed, is composed of a woven KEVLAR®-49/epoxy skin and graphite/epoxy frames and stringers. The single cure concept is made possible by the utilization of pre-molded foam cores, over which the graphite/epoxy pre-impregnated frame and stringer reinforcements are positioned. Bolted composite channel sections were selected as the otpimum joint construction.

To support the selection of this specific design concept a materials study was conducted to develop and select a cure compatible graphite and KEVLAR-49/epoxy resin system, and a foam system capable of maintaining shape and integrity under the processing conditions established. The materials selected were, Narmco 5209/Thornel T-300 graphite, Narmco 5209/KEVLAR-49 woven fabric, and Stathane 8747 polyurethane foam.

---

* The contract research effort which has led to the results in this report was financially supported by USAAMRDL (Langley Directorate).

A manufacturing study, which included visits to various airframe manufacturers engaged in the fabrication of composite hardware, was conducted to evaluate and select tooling concepts applicable to the chosen fabrication concept. Both steel plate and high temperature epoxy sandwich structure female tools constructed to the outside mold line (OML) were initially selected for evaluation, however the dimensional stability of the steel tool proved superior and steel tooling was used for the remainder of the program.

Eight specimens were fabricated, representative of the frame, stringer, and splice joint attachments. Evaluation of the results of analysis and test indicate that design predictions are good to excellent except for some conservatism of the complex frame splice.

This report summarizes the work accomplished in Phase I of a two phase effort. During Phase II of the program, the materials, procedures, and tooling concepts developed in this phase will be utilized in the fabrication of a multi element fuselage section, and dynamic fatigue tests will be performed on individual frame elements cut from this section.

SECTION 1.0 INTRODUCTION

The application of advanced composite materials in the manufacture of development, test, and prototype hardware has been proven successfully many times in the past. Much effort has been directed towards the development of the "ideal" composite structure. Theoretical programs have been developed to the point of sophistication where they can provide to a designer, the orientation, location, combination, and sequence of selected reinforcements, to produce the optimum structure/weight combination.

Production of composite structures will not however, become a reality until simplified manufacturing techniques are developed to produce a truly cost effective article. A simplified manufacturing technique can be developed only when the designer, the materials engineer, the analyst and the producibility experts are integrated into a single team to design and produce composite hardware. In all cases there must be a tradeoff between the "theoretical optimum structure", the "absolute minimum weight structure", and the "lowest cost structure". In a recent preliminary design study (Reference 1), Sikorsky Aircraft has shown, that through a rational design approach in the application of composites to large helicopter airframe construction, cost and weight savings are achievable. One approach, a foam stabilized frame/stringer construction as shown in Figure 1, provides a cost effective solution for composite construction using todays technology.

The objective of this program is to investigate and determine the potential of the foam stabilized frame/stringer concept for producing low cost hybrid composite fuselage components. This study is the Phase I effort of a two phase program, and was directed towards the analysis and design of a producible frame/stringer/skin test element and the evaluation and selection of process compatible constituent materials. It also includes the evaluation and selection of a tooling concept, the fabrication of representative frame and stringer test elements, and the test verification of the static properties of these elements.

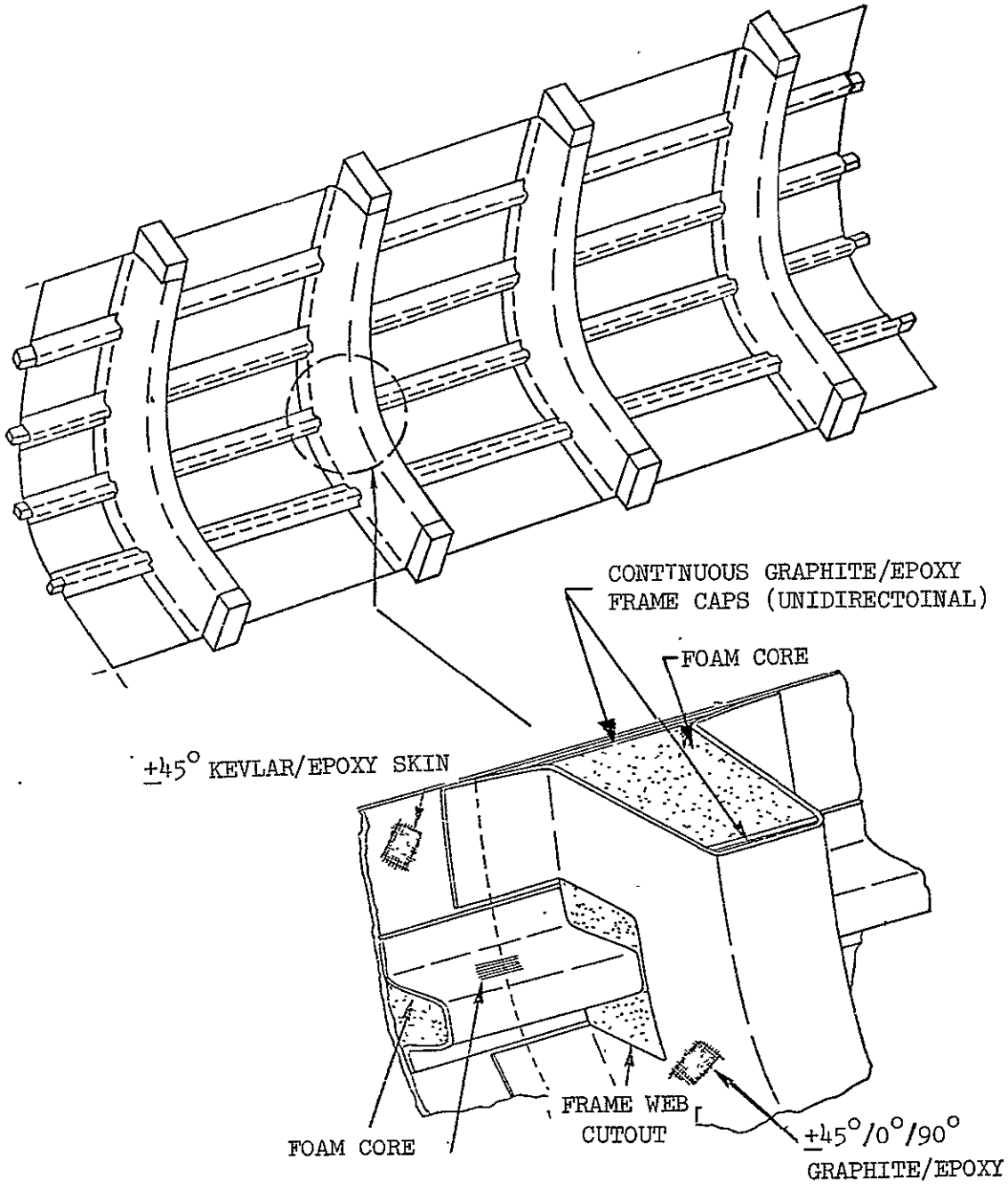

FIGURE 1. INTEGRAL SHELL CONSTRUCTION PROVIDES STRUCTURAL INTEGRITY WITH POTENTIAL FOR SINGLE CURE CYCLE FABRICATION.

SECTION 2.0 DESIGN AND ANALYSIS

The airframe weight breakdown for the CH-53D, a typical current large cargo helicopter, is shown in Figure 2 and reveals that a major portion of the structure is in the aluminum outer shell (skin/stringer/frames) of the cabin section which is designed by strength considerations that include crippling, buckling, and ultimate stress. This region of the airframe is therefore highly suitable for application of the high specific strength of composite materials. Frame and stringer stiffened skin represent the most successful conventional approach to large helicopter construction. Design of a frame/stringer/skin construction of composite materials also appears to provide the greatest weight advantage with the lowest fabrication risk as determined in the Reference (1) program. The analysis for the basic stringer and frame is relatively simple because all loads have been established for the existing production airframe which provides the basis for this design. Therefore the analysis was conducted to verify the adequacy of the basic stringer and frame geometry which had been established in Reference (1). To simplify the frame design for this study, and to determine the practicability of composite fabrication techniques, a typical highly loaded cabin frame with a constant four inch depth was chosen for detail design and fabrication. Analysis of the stringer and frame splice joints involved the selection of various laminate combinations and the determination of safety margins for these combinations. Selection of final laminate configurations were based on the least number of plies necessary to produce a positive margin.

2.1 COMPOSITE SKIN DESIGN

The initial design studies for the selection of the composite skin under Reference (1) indicated that $\pm 45°$, 4 ply graphite-epoxy skins provided more than adequate shear strength and was the lowest weight solution. The design concept was to carry the 1g normal flight loads in an unbuckled mode, and the higher flight and ground loadings in a diagonal tension field (post buckled mode). However impact studies also indicated that the light gage graphite skin required reinforcement with glass-epoxy or KEVLAR-49 (0°/90°) for adequate impact damage tolerance. KEVLAR-49 was selected over glass-epoxy because of its better thermal compatibility with graphite and lower weight. In further design tradeoffs conducted during this program it became apparent that the composite stringer/frames provided a significant increase in rigidity over the usual aluminum construction. This greater rigidity of the composite construction is due to the increased bending properties which result from the foam stabilized hat section configuration. In addition a further review indicated the 1g non buckled criteria was too conservative and was not being used in current helicopter airframe aluminum sheet metal type construction.

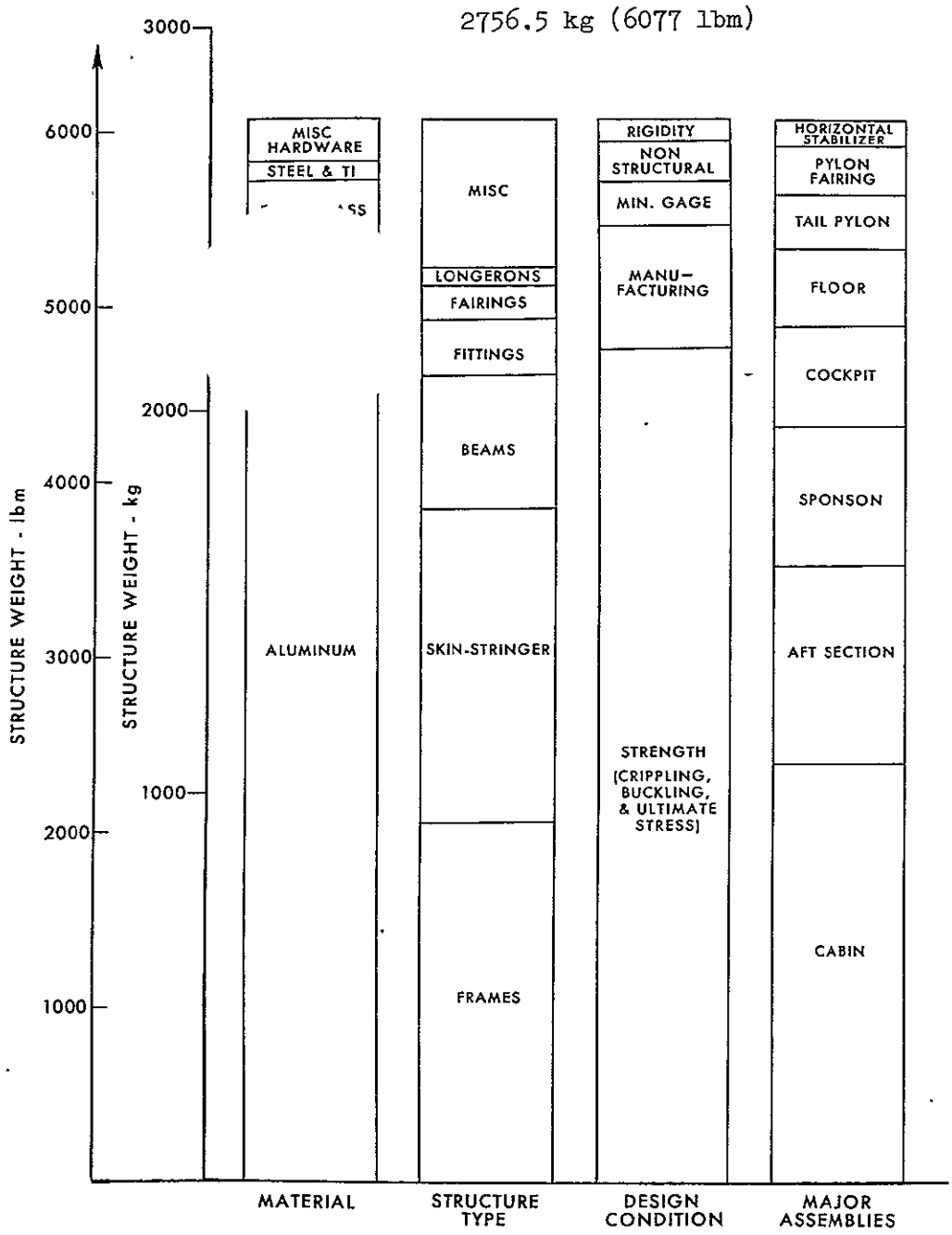

FIGURE 2. CURRENT CH-53D AIRFRAME IS PRIMARILY ALUMINUM ALLOY WITH THE MAJOR WEIGHT IN THE OUTER SHELL CONSTRUCTION.

Thus the combination of the increased rigidity of the composite framing members as compared to current aluminum construction, and the relaxation of the 1g unbuckled criteria, indicated that the skins can be designed completely for the post buckled mode (diagonal tension field). A four ply ±45° woven KEVLAR-49 skin provides more than adequate strength in a diagonal tension field for the design shear loadings of the CH-53, and in addition provides better damage tolerance than the previous construction of graphite and KEVLAR-49. Thus a lighter, lower cost and increased impact damage tolerance structure results from the design selection of KEVLAR-49 for composite skins.

2.2 FRAME DESIGN AND ANALYSIS

In this type of airframe construction, the function of the frame is to maintain the shape of the aircraft, provide stabilizing supports, and termination points for longitudinal stringers. At points where large concentrated loads are introduced, such as at attachment areas for the tail cone, landing gear, transmission, external load carrying provisions etc., relatively heavy frames are used. In general, frames are of such shape, and the load distribution of such a character, that they undergo bending forces in transferring loads to the other resisting portions of the airframe. The bending force distribution around relatively heavy frames is typically 11 298N·m (100,000 in-lbs) for the CH-53D aircraft.

The foam stabilized frame, can be integrated into the integral one step cure frame/stringer/skin concept with no prior fabrication required, other than that of the foam core or support. This provides a great design flexibility in that modification can be incorporated at the time of fabrication to permit the substitution or addition of localized reinforcements to meet users specific requirements. Theoretical weight savings in the order of 33% are calculated. The detail design of the frame/stringer/skin configuration utilized in this study is presented in Figures 3a and 3b.

For this study the frames are considered to be part of an assembly and therefore the frame splices must be designed to carry frame bending loads. To reduce the weight penalty associated with the heavy localized buildups for hardware attachments necessary to provide load transfer in splice areas, the frame splices are located where frame bending loads are minimum. The maximum design loads for the composite frame to be evaluated in this study are 11 298 N·m (100,000 in-lbs) bending, an axial load of 71 168N (16,600 pounds) and a shear load of 44 480N (10,000 pounds). The axial loads and the bending moment are reacted by unidirectional 0° oriented graphite caps, placed as shown in Figure 3a. The total load reacted by the upper cap (107 of Figure 3a) is:

$P_{cap} = (P_c/2)+(M/d)$

Where P_c = Axial load = -16,600 lbs (compression)

M = Bending Moment = -100,000 in-lbs (compression upper cap)

d = distance from centroid of the upper and lower caps - 3.84 in.

P_{cap} = Load in cap (lbs)

$$P_{cap} = \frac{-16,600}{2} + \frac{(-100,000)}{3.84} = -8,300 + (-26,100)$$

$$= -34,000 \text{ lbs (compression)}$$

Area of the upper cap (A_{cap}) is:

$$A_{cap} = .22(2.x.57) = .251 \text{ in}^2$$

The compression stress in the cap (f_c) is:

$$f_c = P_{cap}/A_{cap}$$

$$= 34,400/.251 = 137,000 \text{ psi}$$

The ultimate allowable compression stress (F_{cu}) is 160,000 psi (reference 4) since crippling is not critical

The margin of safety (M.S.) is:

$$M.S. = (F_{cu}/f_c)-1 = (160,000/137,000) -1 = +.16$$

The total load reacted by the lower cap (P_{cap}) (-106 of fig. 3a) is: $P_{cap} = P_c/2 -(M/d)$

$$= -8,300 - (-26,100)$$

$$= +17,800 \text{ lbs (tension)}$$ (Frame is therefore compression critical)

For a reversed bending moment to cause maximum compression in the lower cap, the load would be the same as the upper cap which is 34,400 lbs.

Area of the lower cap (A_{cap}) is:

$$A_{cap} = .1(2 \times .88)+.1(1.62-.88) = .250 \text{ in}^2$$

The compression stress is:

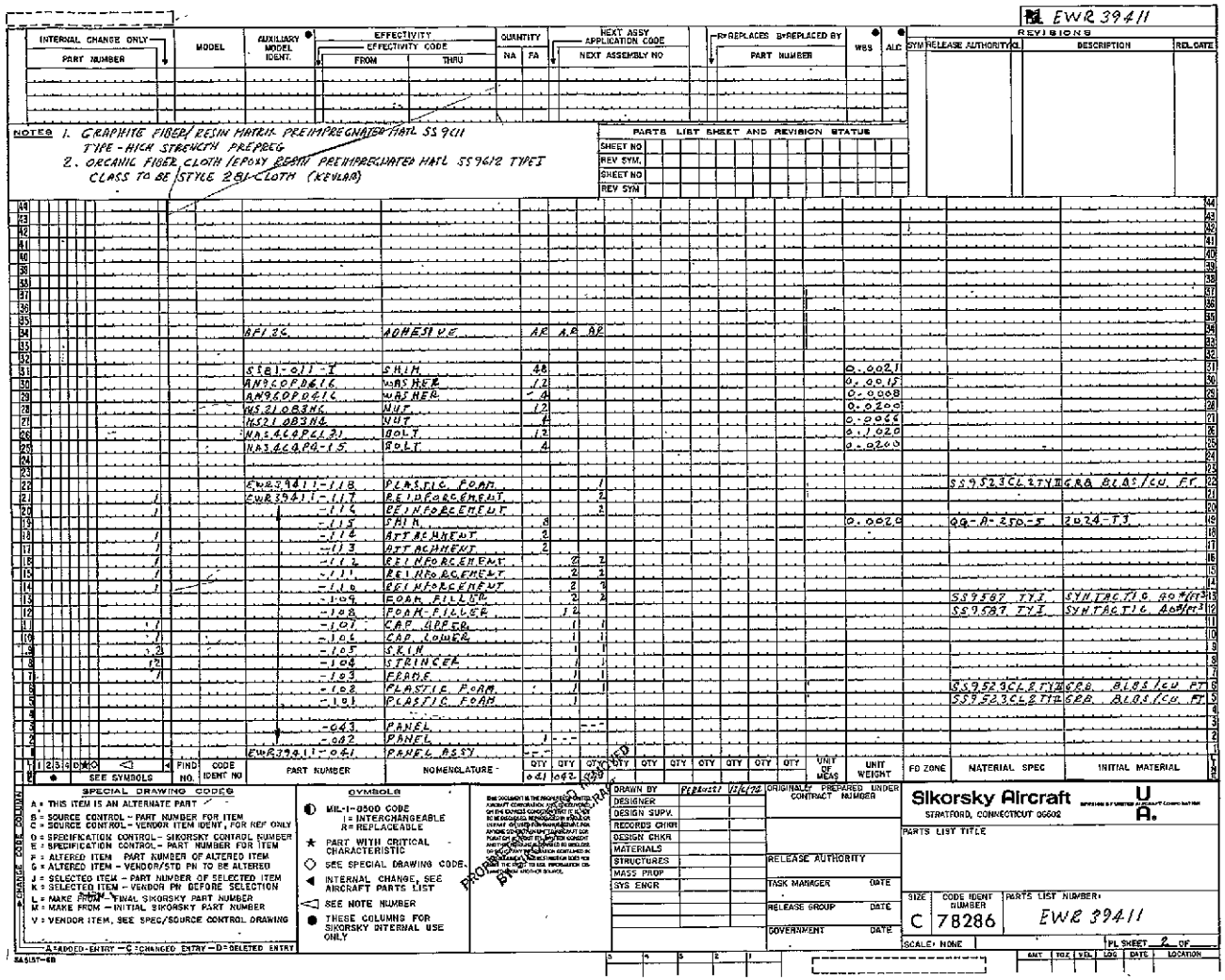

FIGURE 3b. EWR-39411 TEST SPECIMEN DRAWING, SHEET #2.

$$f_c = P_{cap}/A_{cap}$$

$$f_c = 34,400/.250 = 137,600 \text{ psi}$$

Although this value is less than the allowable ultimate compressive stress. The allowable compression stress might be based upon compression buckling of the small tapered flanges of the lower cap which are sandwiched between the web material of the frame and the KEVLAR skins. Since no data is available for such construction, the following is assumed;

b/t = flange width divided by thickness = .74/.125 = 5.7

From figure 11 reference (1) it can be shown that for b/t valves less than 6.5 the allowable crippling stress is equal to the ultimate allowable compression stress (F_{cu}) for the material which is 160,000 psi (reference 4)

Therefore the Margin of Safety (M.S.) = $(F_{cu}/f_c)-1$
$(160,000/137,000)-1 = +.16$

The frame web (103 of Figure 3a) is composed of six plies of graphite epoxy oriented at ±45°, two plies oriented at 0° and two plies oriented at 90°. It is assumed that the ±45° graphite fibers react the shear load on the frame. The shear stress (f_s) on the frame web at the stringer intersection is:

$$f_s = \frac{(V/h)/2}{t}$$

Where V = Shear load = 10,000 pounds

t = Thickness of ±45° plies = .033 in

h = Height of web at stringer intersection = 3.25 in

$$f_s = \frac{(10,000/3.25)/2}{0.033} = 46,200 \text{ psi}$$

The ultimate allowable shear stress (F_{su}) is 50,200 psi (from reference 2).

The Margin of Safety (M.S.) is:

M.S. (Web) $= (F_{su}/f_s)-1 = (50,200/46,200)-1 = +.08$

The 0° and 90° graphite fibers are used to provide reinforcement for the web where the continuous stringer passes through the web. Shear buckling of the web is not a design problem since the web is more than adequately stabilized by the

foam core.

2.3 STRINGER DESIGN AND ANALYSIS

The stringers must be capable of reacting primary axial loads due to airframe bending plus induced compression axial loads due to diagonal tension effects of post buckled skins. When designed in combination to utilize their combined loading strength, the foam stabilized stringer/skin provides a higher strength capability, and a higher combined load strength to weight ratio, than conventional C section stringer and skin construction. The critical load in a typical stringer is the compression load which can vary from 6 672N (1,500 pounds) to 22 250N (5,000 lbs). The design compression load for the composite stringer at a column length of 50.8 cm. (20 inches) is 13 344N (3,000 pounds) due to fuselage bending, and an assumed additional load of 6 672N (1,500 pounds) due to buckled skins. The additional loading from the buckled skins applies only to the stringer but not for end joints.

Section properties of the stringer selected for fabrication (-041 stringer test element, Figure 3a) are as follows:

$A = .066\ in^2$ (0° Graphite Epoxy)

$A = .030\ in^2$ (±45° KEVLAR Epoxy)

$A_{total} = .096\ in^2$

$I_{xx} = .0057\ in^4$ (0° Graphite Epoxy)

Because the compression allowable for ±45° KEVLAR is considered negligible only the graphite is considered.

The critical column load (P_{cr}) for the stringer is:

$$P_{cr} = \frac{C\,\pi^2 EI}{L^2}$$

Where C = Column fixity = 2

E = Modulus of 0° Graphite/Epoxy = 17×10^6 psi

L = Column length = 20 inches

Therefore $P_{cr} = \frac{2\pi^2 \quad (17 \times 10^6)\ .0057}{20^2}$

$P_{cr} = 4{,}790$ pounds

P_c = Design compression load = 4,500 lbs

The Margin of Safety (M.S.) is:

$$\text{M.S. (Column)} = (P_{cr}/P_c) - 1 = (4{,}790/4{,}500) - 1 = +.06$$

Local crippling stringer to skin flange:

$$F_{crippling} = \frac{F_{cu\ G/E}\ A_{G/E} + F_{cukev}\ A_{kev}}{A_{G/E} + A_{kev}}$$

Where $F_{cu\ G/E}$ = Compression Allowable For 0° graphite/epoxy
= 160,000 psi (from reference 2)

$A_{G/E}$ = Foam stabilized area for graphite/epoxy
= .044 in^2

F_{cukev} = Compression Allowable for Kevlar, where b/t = 22, = 20,000 psi (from reference 1 figure 11)

A_{kev} = Foam stabilized area for kevlar
= .022 in^2

$$F_{crippling} = \frac{160{,}000 \times .044 + 20{,}000 \times .022}{.044 + .022}$$

$$= 107{,}000 \text{ psi}$$

$$P_{crippling} = F_{crippling} \times A_{total} = 107{,}000 \times .066 = 7{,}070 \text{ lbs}$$

P_c = Design compression load = 4,500 lbs

The Margin of Safety (M.S.) is:

$$\text{M.S. (Crippling)} = (P_{crippling}/P_c) - 1 = (7{,}070/4{,}500) - 1 = +.57$$

It should be noted that while the crippling margin is much higher (than for column action) there is less confidence for the crippling allowables.

2.4 STRINGER AND FRAME JOINT ANALYSIS

Both the stringer and frame are the same general shape, and the simplest design concept for an attachment splice was considered to be an external fitting, fitted over and attached with bolts to the joining frames or stringers upon assembly. The shape of the fittings, shown in Figures 3a, and 4 provides an allowance for manufacturing misalignment between joining members. Selection of the composite hat section fitting eliminates the problems associated with the co-curing of metallic fittings and the complex and extensive tooling required to insure matching alignment of joining structures.

The maximum design load for the stringer splice is 13 344N (3,000 pounds) in axial compression. The frame splice is designed to withstand 14 678N (3,400 pounds) in axial compression and 2 260 N·m (20,000 in-lb) bending. To determine the mechanical attachment locations, and the laminate configuration for the frame and stringer joints, the strength of the stringer and frame joints were analyzed with the aid of a modified version of a computer program developed at Carnegie-Mellon University for the analysis and optimization of mechanically fastened joints in composite materials. (Reference 3). This program provides a rapid analysis capability for axially loaded joints with the assumption of rigid bolts. The stress analysis in the program is based on the complex stress function method. The joint strength analysis is based on comparing the calculated stresses at the bolt hole in each layer of the composite laminate with the allowable stresses for the material. Experimental data (Reference 3) indicates that this type of strength analysis tends to be conservative.

Stringer Joint

The basic dimensions of the stringer joint are shown in Figures 3a and 4b. This joint contains four 6.35mm (.250 in.) diameter bolts, and it is subject to a maximum axial load P = 13 344N (3,000 pounds). A flat plate model of this joint was defined as shown in Figure 5 in order to apply the Carnegie-Mellon computer program. The computer program was then run with various numbers of 0° and ±45° graphite-epoxy plies in order to find the best laminate design. The graphite-epoxy properties used in this analysis were obtained from Reference 2. The results of the analysis are shown in Table I. The predicted loads at which first fiber failure and first matrix failure occur were calculated and used to determine margins of safety for each condition. Any fiber failure usually results in total joint failure, whereas matrix failure is generally not catastrophic. Based on the results shown in Table I, joint Number 8 containing 8 plies at 0° and 8 plies at ±45° (total of 16 plies) was chosen for the final design. The margin of

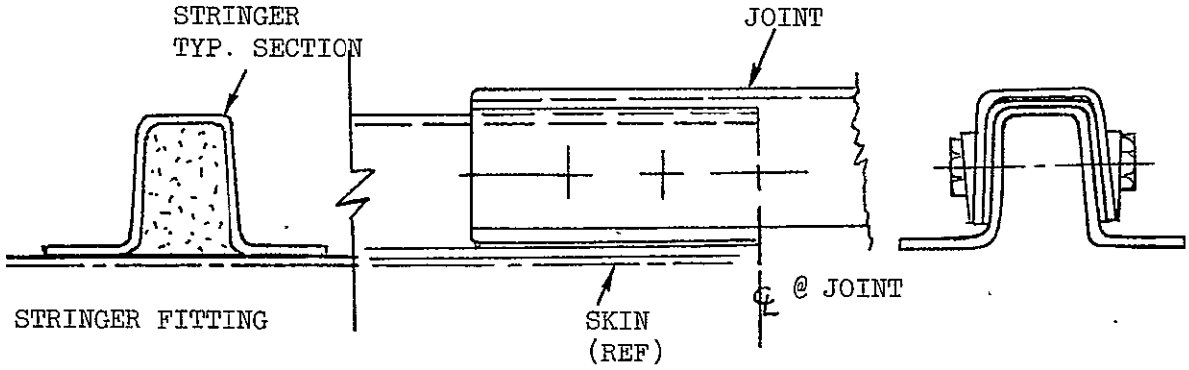

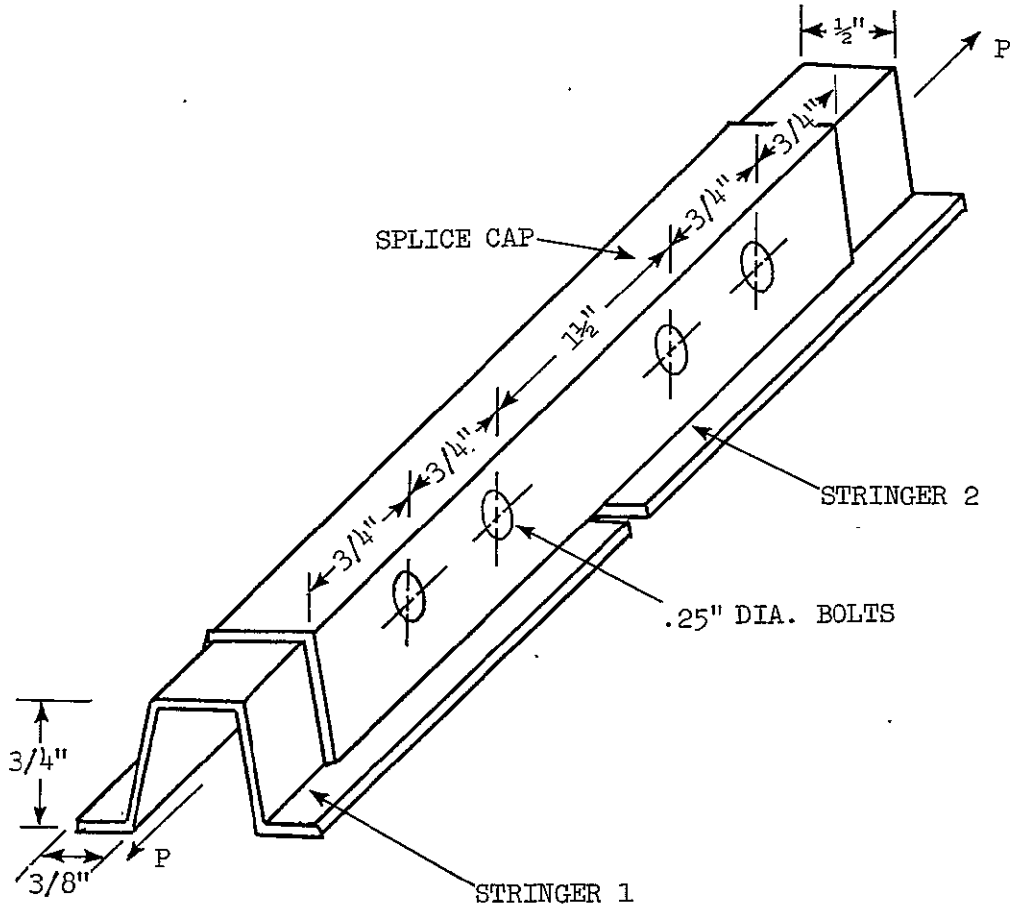

FIGURE 4. COMPOSITE STRINGER JOINT SPLICE CAP.

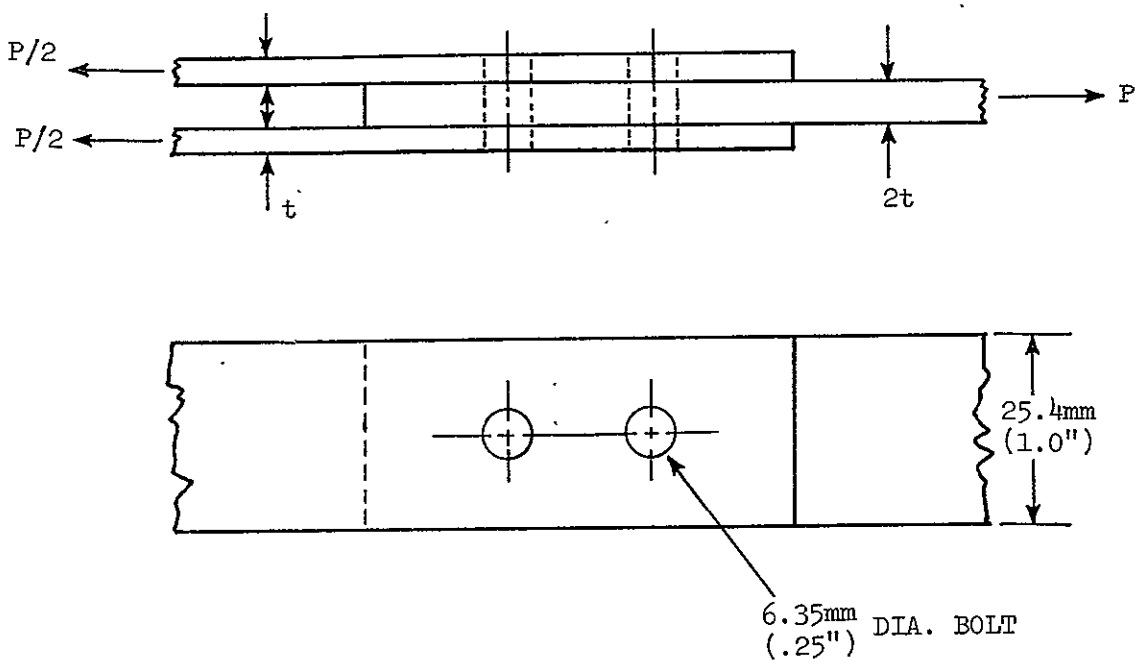

FIGURE 5. FLAT PLATE MODEL FOR ANALYSIS OF STRINGER JOINT.

TABLE I

ANALYSIS RESULTS FOR STRINGER JOINT

APPLIED LOAD P = 13 344N (3000 LBS)

JOINT NUMBER	1	2	3	4	5	6	7	8	9
NO. OF 0° PLIES THICKNESS 0° PLIES	12 1.68 mm (.066 in)	12 1.68 mm (.066 in)	12 1.68 mm (.066 in)	10 1.40 mm (.055 in)	10 1.40 mm (.055 in)	10 1.40 mm (.055 in)	10 1.40 mm (.055 in)	8 1.12 mm (.044 in)	8 1.12 mm (.044 in)
NO. OF ±45° PLIES THICKNESS ±45° PLIES	8 1.12 mm (.044 in)	6 0.84 mm (.033 in)	4 0.56 mm (.022 in)	10 1.40 mm (.055 in)	8 1.12 mm (.044 in)	6 0.84 mm (.033 in)	4 0.56 mm (.022 in)	8 1.12 mm (.044 in)	6 0.84 mm (.033 in)
TOTAL NO. OF PLIES TOTAL THICKNESS	20 2.79 mm (.110 in)	18 2.51 mm (.099 in)	16 2.24 mm (.088 in)	20 2.79 mm (.110 in)	18 2.51 mm (.099 in)	16 2.24 mm (.088 in)	14 1.96 mm (.077 in)	16 2.24 mm (.088 in)	14 1.96 mm (.077 in)
MARGIN OF SAFETY * FIBER FAILURE MODE	+.47 T	+.36 T	+.19 T	+.41 T	+.30 T	+.19 T	+.05 T	+.13 T	+.02 T
MARGIN OF SAFETY* MATRIX FAILURE MODE	+.14 SP	-.08 SP	-.32 SP	+.37 SP	+.11 SP	-.13 SP	-.33 SP	+.10 SP.	-.16 SP

* FAILURE MODES:

T = NET TENSION FAILURE (CRITICAL)

SP = SPLITTING OF MATRIX (NOT CRITICAL)

safety (M.S.) for the matrix failure mode is +.1.

Frame Joint

The basic dimensions of the frame joint are shown in Figures 3a and 6. This joint contains twelve 9.52mm (.375 in) diameter bolts, and it is subject to a maximum axial load of 15 122N (3,400 pounds) and a maximum bending moment of 2 260 N·m(20,000 in-lbs). An accurate analysis of a joint subject to axial and bending loads requires a detailed finite element analysis, which was beyond the scope of this program. An approximate analysis of this joint was therefore conducted with the aid of the Carnegie-Mellon program. For the approximate analysis the applied loads and distribution of bolt loads on the splice cap was assumed to be as shown in Figure 7. This bolt load distribution was obtained by assuming that the loads resulting from the bending moment were proportional to the distance to the center of the bolt pattern, and acted perpendicular to a line extending from the bolt to the center of the bolt pattern. The bolt loads resulting from bending are therefore given by the equation:

$$P_{Bmi} = \frac{Mr_i}{\Sigma r_i 2}$$

Where P_{Bmi} = bolt load on i^{th} bolt resulting from the bending moment

M = applied bending moment

r_i = distance from center of bolt pattern to i^{th} bolt

The axial load was assumed to be equally distributed between the outer four bolts (i.e. bolts numbers 1,3,4 and 6 in Figure 7).

An examination of Figure 7 indicates bolt number 1 to be the most highly loaded bolt, since it is subject to the highest bolt loads plus a tensile bending stress produced by the load introduced at bolts number 2,3,5 and 6. A modified version of the Carnegie-Mellon program was used to obtain approximate stresses around bolt hole 1 resulting from the bolt load and incoming tensile load. These stresses were superimposed and the total stress was input to a computer program for the analysis and design of fibrous composite laminates in order to perform the strength analysis.

The simple plate models used to obtain the stresses resulting from the incoming tensile stress and the bolt load are shown in Figure 8a and 8b respectively. The incoming plate stress is

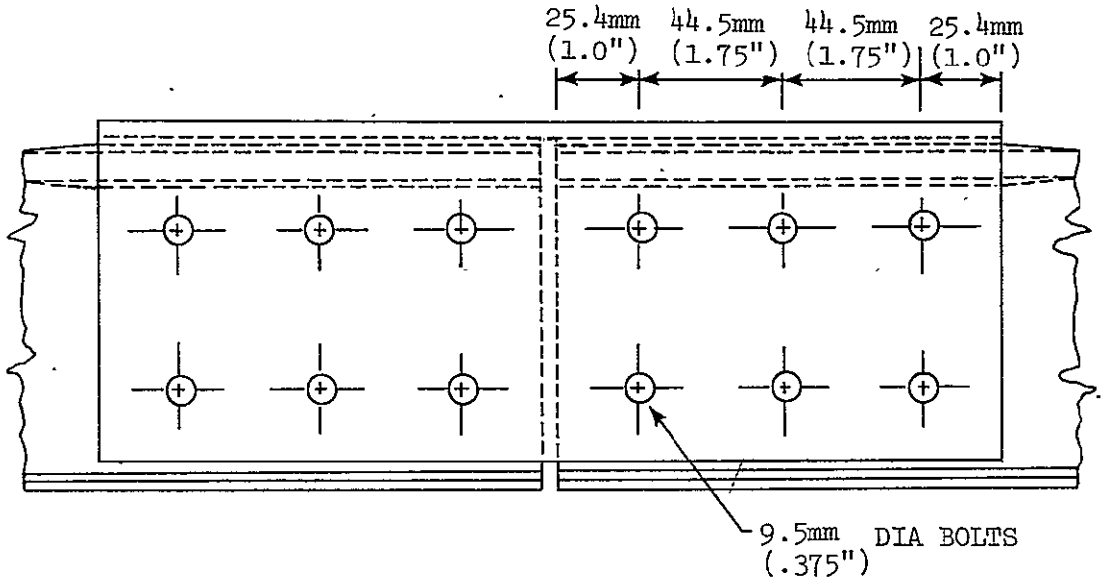

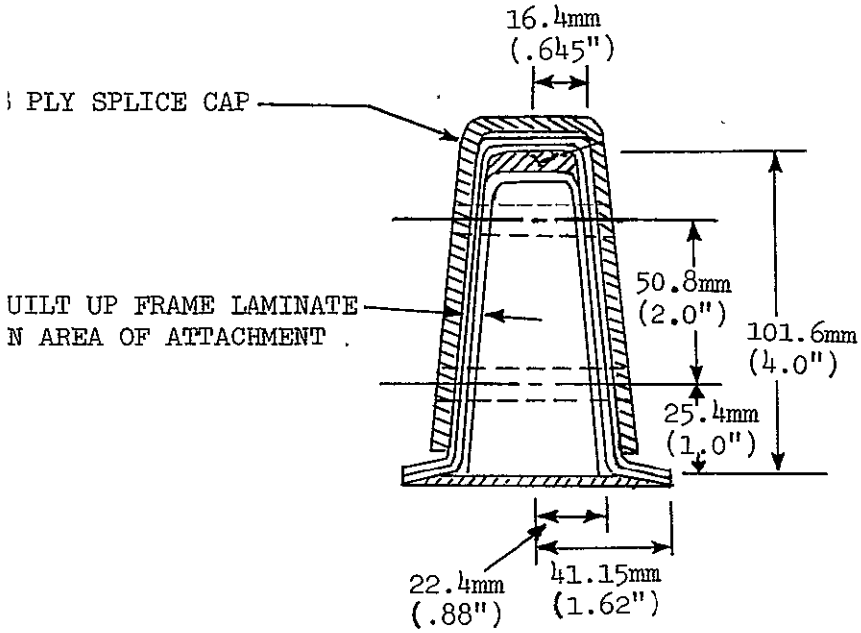

FIGURE 6. COMPOSITE FRAME JOINT SPLICE CAP CONCEPT.

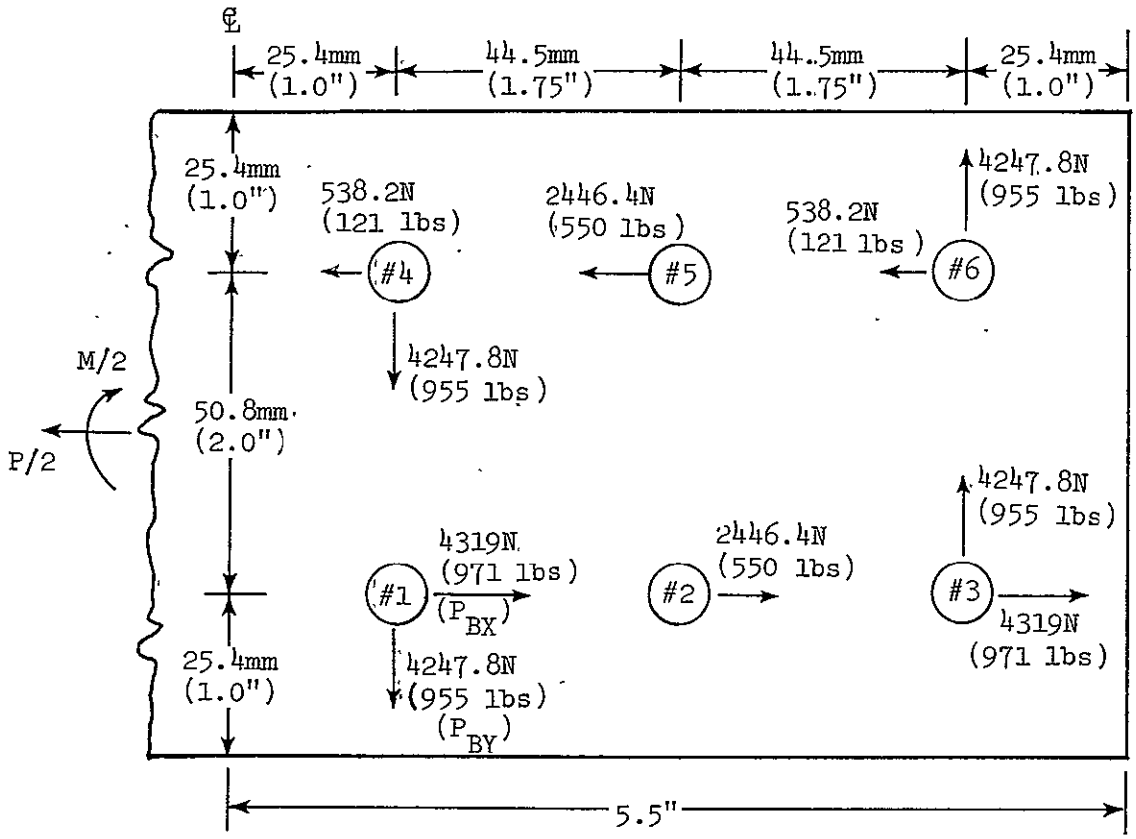

M = 11 298 N·m (20,000 in.-lbs)
P = 15123.2N
(3400 lbs)

FIGURE 7. · FRAME JOINT, MODEL OF ONE SIDE OF SPLICE CAP SHOWING BOLT LOADS.

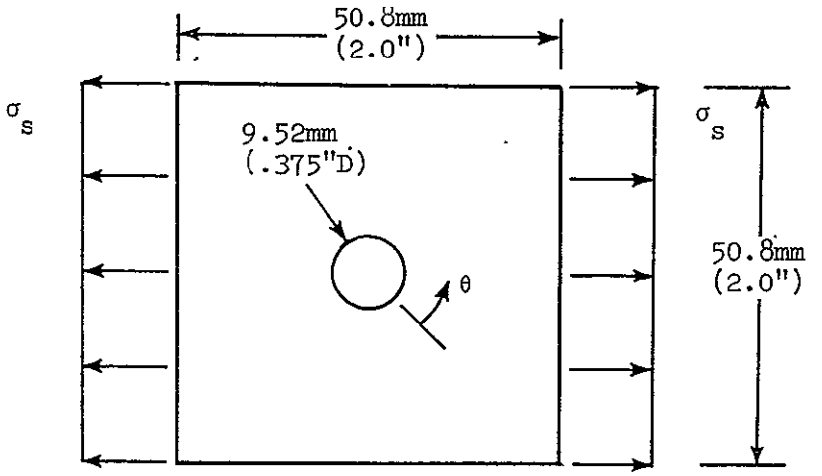

(a) MODEL FOR INCOMING STRESS FROM OTHER BOLT LOADS

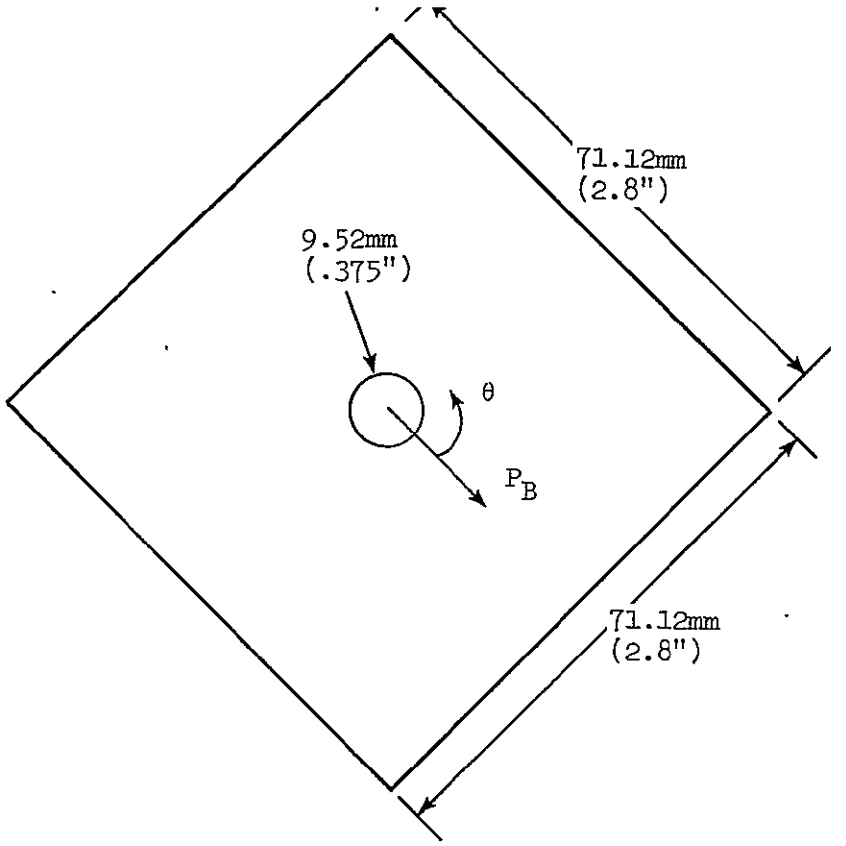

(b) MODEL FOR BOLT LOAD

FIGURE 8. PLATE MODELS FOR FRAME JOINT.

calculated from the equation:

$$\sigma_s = \frac{MY}{I} + \frac{P}{A}$$

Where M = 5,535 in-lbs = moment produced by bolts 2,3, 5 and 6 in Figure 7.

Y = 1.5" = distance from neutral axis of splice cap to furthest point on bolt 1 in Figure 7.

I = 13.51 t = moment of inertia of splice cap (t = unkown splice cap thickness)

P = 850 pounds = axial load produced by bolts 2,3,5 and 6 in Figure 7

A = 9.29 t = cross section area of splice cap (t = unkown splice cap thickness)

The bolt load P_B = 1,400 pounds is the resultant load acting on bolt number 1 in Figure 7. This load is obtained from the equation:

$$P_B = \sqrt{P_{BX}^2 + P_{BY}^2} = \sqrt{(971)^2 + (955)^2} = 1,400 \text{ pounds}$$

The results of an analysis for a $[0°/\pm45°/90°]_t$ graphite-epoxy laminate containing 32 plies is shown in Table II. The properties of the graphite-epoxy used in this analysis are taken from Reference 4. Table II shows the stress at the bolt hole as calculated by the Carnegie-Mellon program. The stress components σ_{xs}, σ_{ys}, τ_{xys} result from the incoming plates stress

s = 27.58 MPa (4,000 psi) produced by the other bolts, and the stress components σ_{xb}, σ_{yb}, τ_{xyb} result from the bolt load

P_b = 6,227N (1,400 pounds). The total stress components σ_{xt}, σ_{yt}, and τ_{xyt} are the sum of the plate and bolt load stresses.

The margins of safety are obtained by introducing the total stress components into the laminate analysis program. The margins of safety in the line labeled CF are for failure modes that should result in complete joint failure. The margins of safety on the line labeled FF are for first ply failure. Since all margins of safety in Table II are positive and the strength analysis tends to be conservative, a laminate containing 28 plies with a lay up similar to (0°/±45°/90°) was chosen for the frame joint. The failure load for the 28 ply design is estimated by ratio of the number of plies. Based on first ply failure the M.S. (Margin of Safety) is reduced to +.12 for the 28 ply design selection. This criteria is based on having no

TABLE II

ANALYSIS RESULTS FOR FRAME JOINT
32 PLIES $\left[0^{\circ}/\pm 45^{\circ}/90^{\circ}\right]_T$ GRAPHITE-EPOXY

STRESSES @ BOLT HOLE		θ = LOCATION AROUND BOLT HOLE (REFERENCE FIG.8)		
		$\theta = 0^{\circ}$	$\theta = 45^{\circ}$	$\theta = 90^{\circ}$
FROM BOLT LOAD (AVERAGE)	σ_{xb}	-148.6 MPa (-21,549 psi)	8.3 MPa (1,202 psi)	193.0 MPa (27,937 psi)
	σ_{yb}	67.0 MPa (9,271 psi)	-54.3 MPa (-7871 psi)	-3.72 MPa (-539 psi)
	τ_{xyb}	0	-81.4 MPa (-11,814 psi)	38.4 MPa (5,564 psi)
INCOMING FROM OTHER BOLTS (AVERAGE)	σ_{xs}	0	-13.1 MPa (-1,897 psi)	24.9 MPa (3,615 psi)
	σ_{ys}	24.9 MPa (3615 psi)	-13.7 MPa (-1,987 psi)	0
	τ_{xys}	0	13.1 MPa (1,897 psi)	0
TOTAL	σ_{xt}	-148.6 MPa (-21,549 psi)	-4.8 MPa (-695 psi)	217.5 MPa (31,552 psi)
	σ_{yt}	91.9 MPa (13,336 psi)	-67.3 MPa (-9,768 psi)	-3.7 MPa (-539 psi)
	τ_{xyt}	0	-68.4 MPa (-9,917 psi)	38.4 MPa (5,564 psi)
MARGIN OF SAFETY	CF	0.87	2.00	0.89
	FF	0.65	1.84	0.29

CF = COMPLETE FAILURE OF JOINT

FF = FIRST PLY FAILURE

damage up to design ultimate load. For complete joint failure the Margin of Safety is reduced to +.63 for the 28 ply design selection. It is necessary to provide a high Margin of Safety for the joint failure to meet the localized damage failure.

2.5 FATIGUE CONSIDERATIONS

The fatigue of the airframe falls generally in the low to intermediate cycle range (10^3 to 10^6 cycles) and is induced from the air-ground-air (GAG) cycles. G-A-G cycling has not been found to be a problem for the aluminum airframes of helicopters. However a review is required for composite material applications.

In general, the superior fatigue to static strength of composites particularly for stress concentrations indicates no design problems for the composite structures. A comparative ratio of mean fatigue strength for aluminum (Al) and graphite/epoxies (G/E) is:

Material	Ratio Fatigue Strength* to Static Strength	Reference
2024-T3 Al (K_t=1)	.56	Fig.3.2.3.1.8(b),Ref.4
2024-T3 Al (K_t=5)**	.17	Fig.3.2.3.1.8(f),Ref.4
0° G/E (K_t = 1)	.53	Fig.1.2.5-21,Ref. 2
0° G/E (K_t = 3)	.84	Fig.1.2.5-21,Ref. 2
0°/±45° G/E (K_t = 1)	.75	Fig.1.2.4-23,Ref. 2
0°/±45° G/E (K_t = 3)	.94	Fig.1.2.4-23,Ref. 2

* At R = .05, 10^6 cycles
** K_t = 5 is representative for airframe with fretting at riveted joints.

Therefore no increased Margins of Safety are used for static strength of composite to meet fatigue requirements of the airframe structures.

SECTION 3.0 MATERIALS EVALUATION

The selection of all constituent materials for fabrication of composite hardware for any low cost fabrication technique is dependent on the process selected. The incorporation of individual stringer, frame and skin elements into a single hybrid composite structure, presents the potential for significant cost savings to be realized in the manufacture of large helicopter airframe components. To facilitate fabrication of such a structure certain material and process parameters had to be established. The following criteria for the selection of the component materials utilized in this program was based on the premise that it would be feasible to successfully combine, in a single cure, single lay-up operation, composite frames and stringer elements with a composite skin, to form a large integrally reinforced helicopter fuselage section.

3.1 LAMINATE MATERIALS SELECTION

For the primary reinforcement to be used in the frame and stringer elements, Thornel 300 graphite was chosen. Laminates produced with Thornel 300 graphite exhibit higher and more consistent properties than that of the A-S type graphite. Dimensional tolerances of large ply stackings, such as found in attachment areas, can be held more closely, with a greater overall uniformity. This is due to the manufacturing process by which the continuous fiber now is produced. The material also has the greatest potential, among the currently produced high strength graphite fibers, for becoming less expensive.

KEVLAR-49 type III, Polyaramid fiber, was chosen in the form of a woven fabric (style 281) for the skin material because of its superior specific properties over glass and its compatible thermal characteristics with the primary (graphite) reinforcements.

Selection of a resin system suitable for impregnation of both the T300 graphite and the Kevlar-49 Polyaramid was based on:

a) Compatability between, or duplicity of, available system(s) for coating the selected reinforcing fibers.
b) The lowest available cure temperature for the selected system(s) consistent with a minimum heat distortion temperature of 73.88°C (165°F). (The upper environment operating temperature limit of a large transport type helicopter.) A 121.1°C (250°F) cure system was established as a maximum target temperature system.
c) The lowest pressure at which the system could be cured to provide a low void laminate with a fiber volume fraction of at least 50%.
d) Cost of material and availability. Cost of production

material is projected to be proportional to quantities required for the program and cost consideration at this time is the criteria for being within the contract budget. Material must be available within the time frame of the contract requirement.

e) Manufacturing experience, as gained by Sikorsky and other Aerospace manufacturers engaged in similar programs.

Seven candidate suppliers were contacted to determine the availability of candidate systems meeting all of the above established requirements. Of the seven suppliers, only four replied affirmatively as being able to supply materials meeting the established requirements.

Of the four material suppliers, only two indicated the availability of a resin system meeting the 121.1°C (250°F) target cure temperature, Narmco 5209 and Reliable RAC6250. 3M Company recommended a cure temperature of 148.9°C (300°F) for their SP-288 resin system and Ferro/Cordo specified a 135°C (275°F) cure temperature for their E-293 resin system.

See Table III for summary of candidate prepreg materials. Three candidate suppliers were selected for the materials screening evaluation. Two of the three suppliers proposed one resin system for impregnating both the graphite and the KEVLAR-49; Narmco, their 5209, and Ferro/Cordo, their E-293. 3M Company proposed a compatible system, consisting of their SP-288 resin system impregnated on the graphite, and a Narmco resin, 3203 impregnated on the KEVLAR-49. See Table IV for summary of selected candidate laminate/resin systems.

The process variables established for evaluation of the three candidate materials are: Positive pressure cure at .17MPa (25psi) and .34MPa (50psi) and vacuum pressure cure at atmospheric pressure. Cure of the .17 MPa (25 psi) and .34MPa (50 psi) panels was effected in an autoclave, while the vacuum pressure panels were cured in an oven. The cure cycles developed for the three candidate materials are shown in Figure 9.

The test laminates were designed to be representative of a typical stringer laminate configuration and consisted of a balanced laminate with ten plies of T-300 graphite and two plies of KEVLAR-49 oriented as follows: $(0°_5/\pm 45°)_s$.

Nine test laminate panels were prepared, three panels of each of the candidate systems. One panel of each system was processed at .345MPa (50 psi), one at .172MPa (25 psi), and one at vacuum pressure. The fabricated panels were machined into standard specimen configurations for flexural and short beam shear tests. Flexural properties were determined in accordance with ASTM D790, and shear properties in accordance with ASTM

TABLE III

REQUEST FOR COMPATIBLE GRAPHITE/KEVLAR SYSTEM
SUMMARY OF VENDOR REPLIES

VENDOR	SYSTEM DESIGNATION	CURE TEMP.	PRESSURE	MANUFACTURING EXPERIENCE	CO-CURE	AVAILABILITY
1. NARMCO MAT'LS DIV.	GRAPHITE 5209/T300 KEVLAR 5209/281	121°C (250°F)	AUTOCLAVE	YES LTV	SAME RESIN SYSTEM	4 WEEKS
2. 3M COMPANY NARMCO	GRAPHITE SP288/T300 KEVLAR 3203/281	149°C (300°F)	VACUUM BAG AUTOCLAVE	YES NORTHRUP YES NORTHRUP	COMPATIBLE	4 WEEKS
3. DUPONT *	GRAPHITE 5147/T300 KEVLAR 5147/T300	177°C 350°F	AUTOCLAVE	YES CONVAIR	SAME RESIN SYSTEM	NO DATE
4. FERRO CORDO DIV.*	GRAPHITE-E293/T300 GRAPHITE-E293/T300/248 KEVLAR-E293/281	135°C (275°F)	VACUUM BAG	YES SIKORSKY	SAME RESIN SYSTEM	5 WEEKS
5. HERCULES	NO 121°C (250°F) CURING GRAPHITE SYSTEM AVAILABLE UNTIL 1975					
6. FIBERITE	NOT INTERESTED IN SUPPLYING 121°C (250°F) SYSTEM TO SIKORSKY					
7. RELIABLE MANUFACTURING	AT TIME OF INQUIRY, RELIABLE WAS IN THE PROCESS OF DEVELOPING NEW TAPE MANUFACTURING MACHINERY, THEREFORE WAS NOT CONSIDERED FURTHER					

* DUPONT HAS NO 121° C (250°F) GRAPHITE OR KEVLAR SYSTEM AVAILABLE WITH SIGNIFICANT INDUSTRY USE.

*FERRO PROPOSED USE OF STYLE #248 HIGHLY UNIDIRECTIONAL WOVEN FABRIC AS AN ALTERNATE TO PURE UNIDIRECTIONAL GRAPHITE ON THE BASIS OF MANUFACTURING HANDLEABILITY AND SUBSEQUENT AVAILABILITY IN BROADGOODS UP TO 60 INCHES WIDE.

TABLE IV

SUMMARY OF SELECTED CANDIDATE

LAMINATE/RESIN SYSTEMS

CANDIDATE LAMINATE/RESIN SYSTEMS	MINIMUM TEMP. CURE	MINIMUM PRESSURE CURE	RESIN SYSTEM PROCESSING	EXPERIENCE LEVEL	CO-CURE CAPABILITY RISK FOR SYSTEM	AVAILABILITY	COST OF PREPREG $/LB	REPORTED STRENGTH &MODULUS 0° (T-300) GRAPHITE EPOXY MODULUS(E)&STRENGTH(σ)-GPa(MSI) SHEAR-GPa (KSI)		
								FLEX	AXIAL	SHEAR
NARMCO 5209 T-300 G/E 5209 KEVALR-49 (281 or 285)	121°C (250°F) Normal 107°C (225°F) with extended cure time	LTV has molded at 50 psi Vacuum pressure curing not yet demonstrated	Limited experience at Sikorsky indicates no problem	LTV using for S-3A spoiler system	LOW	Within Schedule	85 G/E 62 K/E	E 2.04 (297) σ 134.7 (19.5)		.134 (19.5)
3M SP288 T-300 G/E 3203 KEVLAR-49 (281 or 285)	135°C (275°F)	SP288T-300 Molded Successfully at Vacuum Pressure	Unknown	SP288T300 used extensively at Northrop on YF-17	LOW to Medium	Within Schedule	125 G/E 60 K/E	E 1.39 (200) σ 115 (16.5)	E 1.33 (1.90) σ 120 (18)	.098 (14.0)
Ferro Corp. E293 T-300 G/E E293 KEVLAR (281 or 285)	135°C (275°F)	Has been cured at vacuum pressure	Good to excellent Based on experience	Sikorsky has extensive experience using E293 Resin with Fiberglass	LOW	Within Schedule	180 G/E 62 K/E	E 1.71 (245) σ 109 (15.7)	E 1.28 (184) σ 148 (21.1)	.094 (13.4)

NOTES: (1) Initial costs for small lots
(2) Vendor Typical Data for 0° orientation, room temperature

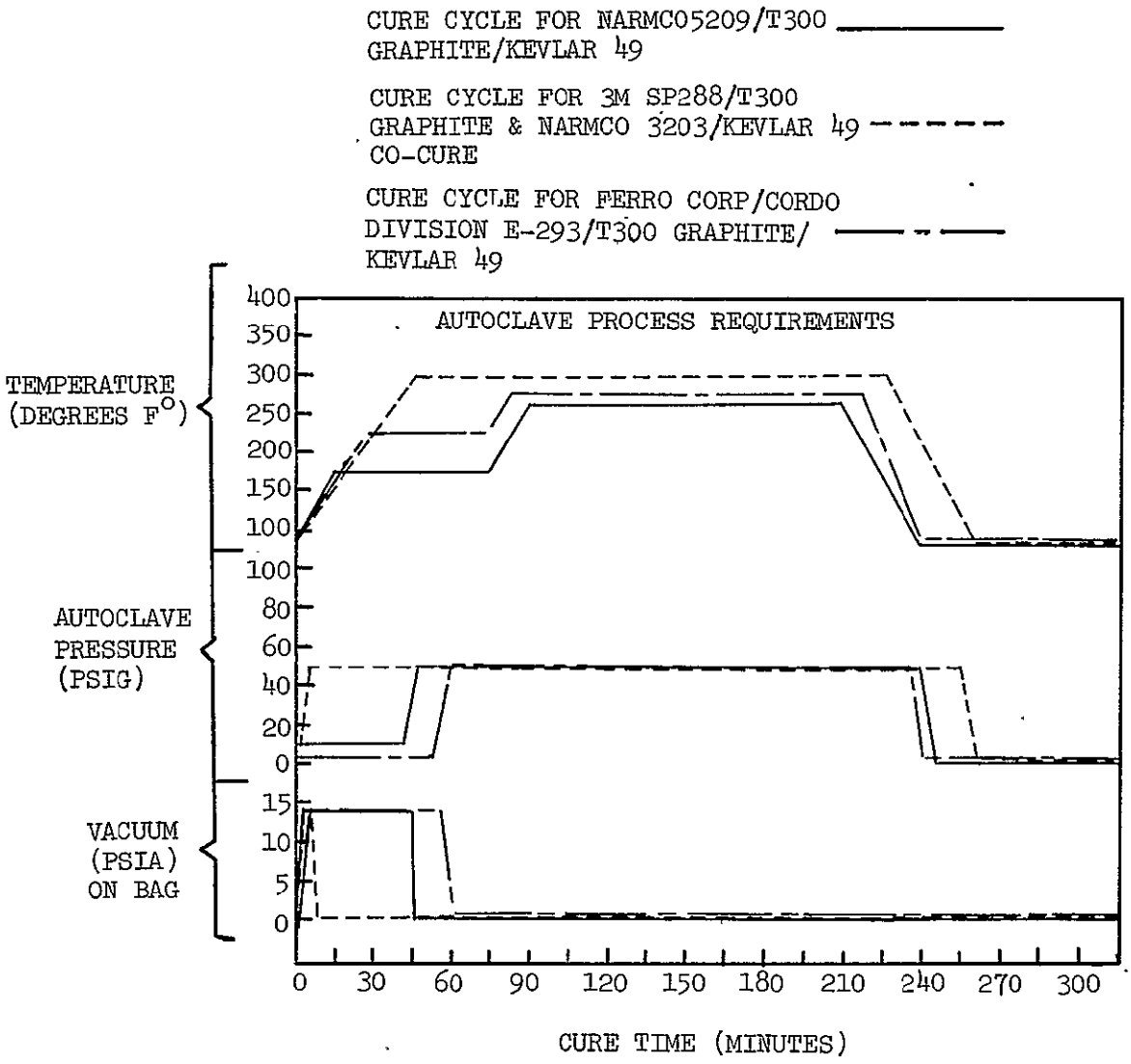

FIGURE 9. CURE CYCLE PROCESS PROFILE CHART, SHOWING SIMILIARITY OF CURE PARAMETERS BETWEEN CANDIDATE RESIN SYSTEMS.

D2344. Results of the flexural and short beam shear tests are presented in Table V. Photomicrographic mounts were prepared for each panel fabricated. As shown in Figure 10, both the 5209/T300/KEVLAR-49 and the E293/T300/KEVLAR-49 at .345MPa (50 psi) are low in void content. The 3M, SP288/T300, NARMCO 3203/KEVLAR-49 co-cure system reveals a high void content in the KEVLAR-49 plies. Although a further investigation was not feasible within the scope of this program, previous investigations of phenomena similar to this indicate the occurrence of a gel time incompatibility between resin systems precluding successful bleedout of the KEVLAR-49 resin. Examination of the panels processed at .172MPa (25 psi) with the exception of higher per ply thickness, reveals the same findings, see Figure 11. All panels cured under vacuum pressure alone, produced laminates with high void contents, with average thickness 6% to 11% higher than those processed at .345MPa (50 psi), See Figure 12. Optimization studies to develop gel time/flow/temperature/pressure relationships were not conducted due to the unavailabiltiy of dialectrometric equipment at the time of fabrication of the evaluation panels. The decision was made, based on the test results, and visual examination of the fabricated laminates, to process all frame/stringer/skin static test specimens at .172MPa (25 psi) vented to atmosphere, using the NARMCO 5209 resin system on both the T-300 graphite and the KEVLAR-49 organic fiber.

3.2 FOAM SELECTION

Since the concept chosen, incorporates the skin, stringer and frame into a single entity, cured in one operation, a mandrel or core is necessary to support and produce the basic shape of the frame and stringer laminates. Extensive experience gained in the search for optimum core materials to be used in the reinforced plastic structures fabricated at Sikorsky Aircraft, such as the cockpit canopy of the CH-53, dictated the use of a rigid polyurethane foam. Literature surveys of the static and fatigue properties of rigid foam systems indicated, that stathane 8747, a CO^2 blown foam with 221 Mg/m^3 (8.0 lb/ft^3) density met the process requirements established for the candidate laminating systems. With a room temperature compressive strength of 1.45 MPa (210 psi) and a 121°C (250°F) compressive strength of 1.31 MPa (190 psi) the Stathane 8747 is ideally suited for autoclave processing. To verify the published data, representative frame core sections were cast, enclosed in a vacuum bag and exposed to actual laminate cure cycles in an autoclave. When exposed to cure temperatures of 177°C (350°F), and a pressure of 0.345MPa (50 psi), with full vacuum maintained during the elevated temperature cycle, the outer cells of the foam collapsed causing a reduction in cross sectional area of approximately 10%. Core sections processed at 121°C (250°F) and a pressure of 0.345MPa (50 psi) with vacuum vented during the initial stage of the cure cycle showed

TABLE V

SUMMARY OF FLEXURAL AND SHORT BEAM SHEAR VALUES
FOR THE THREE CANDIDATE SYSTEMS PROCESSED IN ACCORDANCE
WITH THE PROCESS VARIABLES LISTED

MATERIAL SYSTEM	PROCESS VARIABLE MPa (psi)	LAMINATE THICKNESS mm (in.)	FLEXURE STRESS GPa (ksi)	FLEXURE MODULUS GPa (10^6 psi)	SHEAR MPa (ksi)	COST* GRAPHITE	COST* KEVLAR	COMMENT
NARMCO 5209/T-300 GRAPHITE NARMCO 5209 STYLE 281-KEVLAR 49	.34 (50)	2.03 (0.080)	1.76 (255)	130 (18.8)	87.6 (12.7)	$ 85#	$62#	LOW VOID CONTENT GRAPHITE AND KEVLAR
	.17 (25)	2.08 (0.082)	1.71 (248)	123 (17.9)	88.2 (12.8)			LOW VOID CONTENT GRAPHITE AND KEVLAR
	VACUUM	2.16 (0.085)	1.53 (222)	119 (17.3)	75.8 (11.0)			MEDIUM VOID CONTENT GRAPHITE AND KEVLAR, KEVLAR RESIN RICH
3M-SP-288/T-300 GRAPHITE NARMCO 3203 STYLE 281-KEVLAR 49	.34 (50)	1.83 (0.072)	1.67 (242)	123 (17.9)	88.9 (12.9)	$125#	$60#	LOW VOID CONTENT GRAPHITE, HIGH VOID CONTENT KEVLAR
	.17 (25)	1.93 (0.076)	1.54 (224)	117 (17.0)	89.6 (13.0)			LOW VOID CONTENT GRAPHITE, HIGH VOID CONTENT KEVLAR
	VACUUM	2.03 (0.080)	1.48 (215)	112 (16.2)	80.7 (11.7)			LOW VOID CONTENT GRAPHITE, HIGH VOID CONTENT KEVLAR
FERRO-E293 STYLE 248 T-300 GRAPHITE FERRO-E293 STYLE 285-KEVLAR 49	.34 (50)	2.34 (0.092)	1.61 (234)	129 (18.7)	83.4 (12.1)	$180#	$62#	LOW VOID CONTENT GRAPHITE AND KEVLAR
	.17 (25)	2.59 (0.102)	1.45 (211)	119 (17.2)	82.0 (11.9)			LOW VOID CONTENT GRAPHITE AND KEVLAR
	VACUUM	2.54 (0.100)	1.28 (185)	113 (16.4)	73.1 (10.6)			HIGH VOID CONTENT GRAPHITE AND KEVLAR
DESIGN REQUIREMENT ALLOWABLE			1.10** (160)	117** (17.0)	68.9 (10.0)			

* BASED ON SMALL QUANTITIES PROCURED
** TENSILE

THIS PAGE LEFT INTENTIONALLY BLANK

100X

3M SP-288/T300/NARMCO 3203/KEVLAR 49

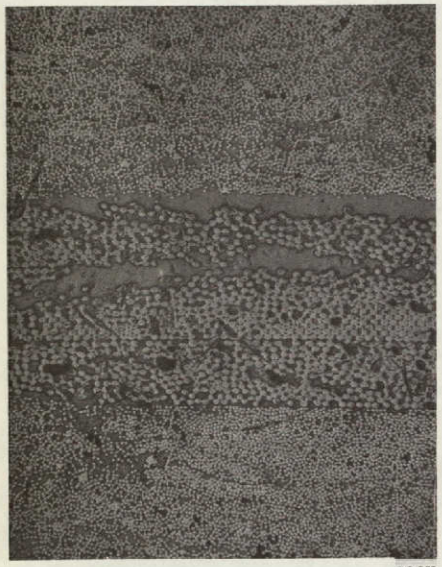

100X

NARMCO 5209/T300/KEVLAR 49

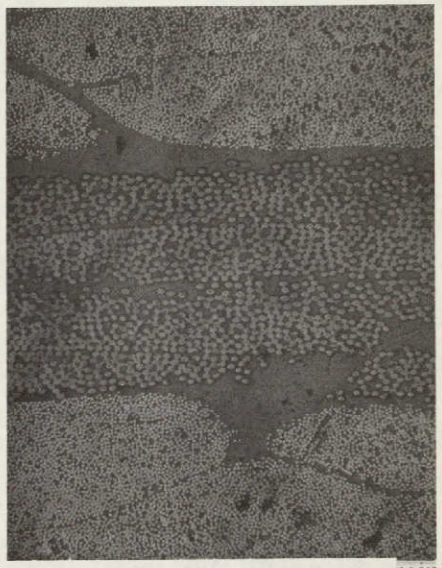

100X

FERRO-CORDO E-293/T300/KEVLAR 49

FIGURE 10. TEST LAMINATE PANELS PROCESSED AT .34MPa (50 psi)

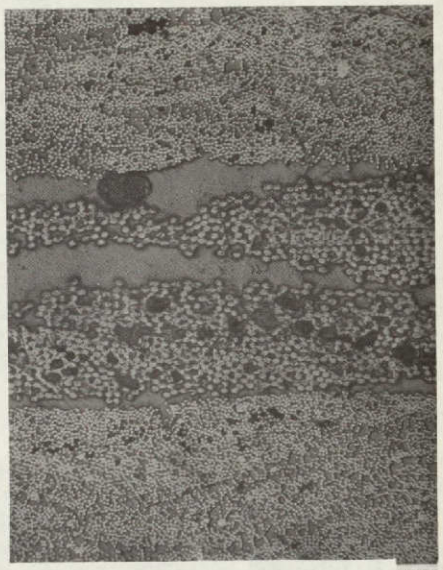

100X

3M SP-288/T300/NARMCO 3203/KEVLAR 49

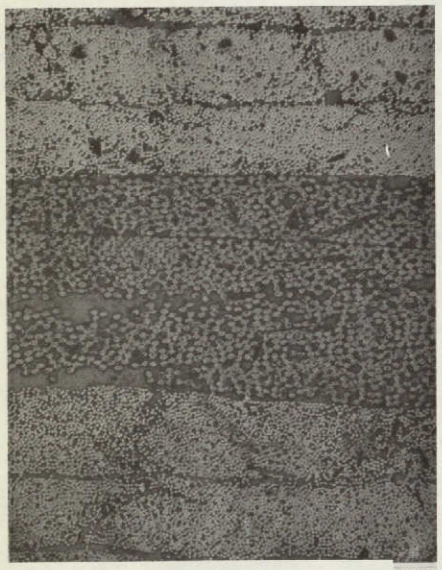

100X

NARMCO 5209/T300/KEVLAR 49

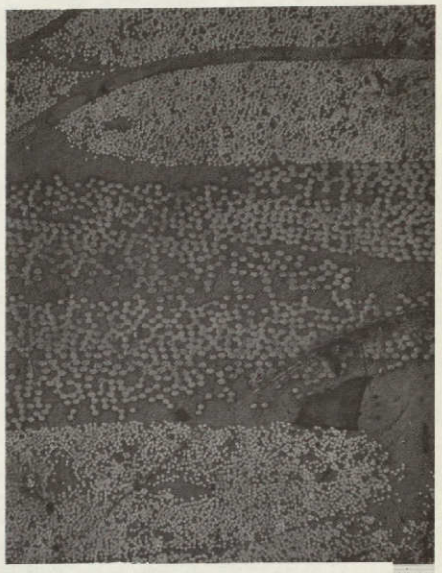

100X

FERRO CORDO E-293/T300/KEVLAR 49

FIGURE 11. TEST LAMINATE PANELS PROCESSED AT .17MPa (25 psi)

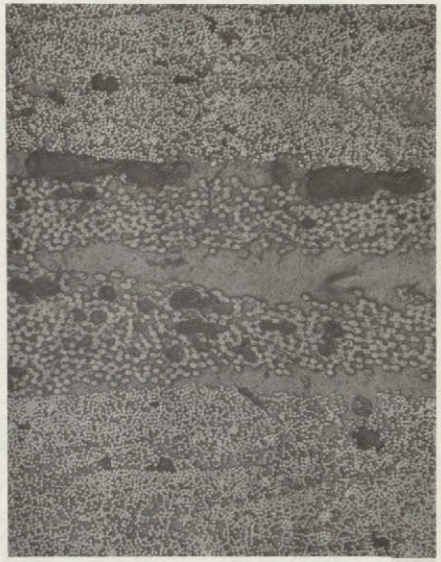

100X

3M SP-288/T300/NARMCO 3203/KEVLAR 49

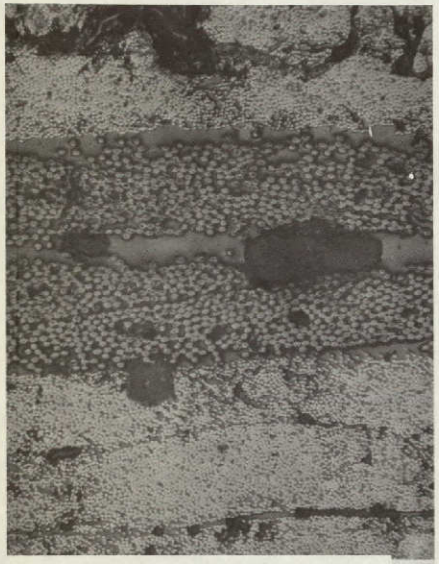

100X

NARMCO 5209/T300/KEVLAR 49

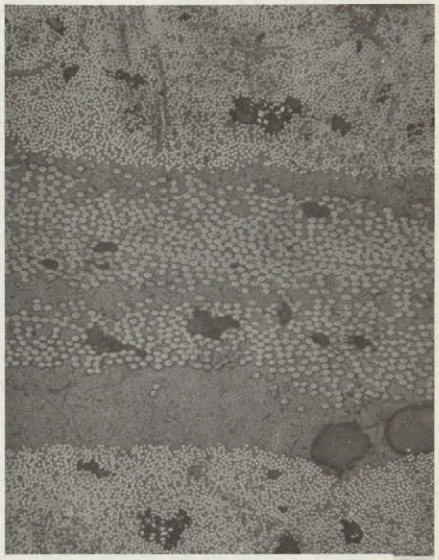

100X

FERRO-CORDO E-293/T300/KEVLAR 49

FIGURE 12. TEST LAMINATE PANELS PROCESSED AT VACUUM BAG PRESSURE.

no measureable distortion. Foam permeability and absorbtion of laminating resin into the outer cells of the core foam was originally considered as a potential problem. In practice, the combination of specific release agents and preheat temperatures of the foam components and foaming tools produces a "self-skin" on the surface of the foam component. The "self-skin" (a surface layer of collapsed cells) produces a surface which is imperveable to the laminating resin.

3.3 PRESSURE TRANSFER EVALUATION

One area of considerable concern in the development of the single cure process was the quality of the stringer laminate where it passes through the frame foam. To evaluate the pressures transmitted to remote areas of the laminate/foam assembly during the curing process, a system of subminiature pressure transducers with a projected capability of fluid pressure measurement in the range of .07-.34MPa (10-50 psi) pressure (model number 500-100) and the attendant pressure indicator (model number System 2100, S/N 183) were purchased from International Technical Industries. Selection of the above system was based on the extremely small size of the transducer sensor, approximately 0.15 cm (0.06 in) in diameter, which would enable the sensor to be incorporated into the laminate during layup of a representative frame/stringer/ skin specimen. Five transducers were installed in the locations shown in Figure 13. Although pressure measurements were recorded during the cure of the specimen, no correlation could be made between the control data and the data recorded during the cure of the actual specimen. Subsequent experimentation revealed that the transducers were more sensitive to the thermal input received during cure, than they were to the pressure transmitted. This thermal screening effect precluded the development of accurate pressure transfer information. With no quantitative values available to verify nondestructively the integrity of the laminate in such inaccessible areas as the frame/stringer intersection, it became necessary to section the part to visually examine the laminate. As shown in Figure 14, pressure transfer through the foam was entirely adequate and good compaction and low void contents were obtained in the stringer. Examination of the upper frame cap laminate exposed during the evaluation of the frame/stringer intersection revealed poor compaction and a large number of voids. Flexural and short beam shear specimens were therefore machined from the upper cap laminate and tested. As expected, flexural strength fell to 1.20 GPa (172,000 psi), modulus to 104.7 GPa (15×10^6 psi) and shear strength to .073 GPa (10,500 psi). Even though these values were above the design allowables it was decided to revise the process parameters selected and establish .345MPa (50 psi) as the pressure requirement for all subsequent processing of specimens, and to include a debulking operation to achieve good overall compaction and bleedout.

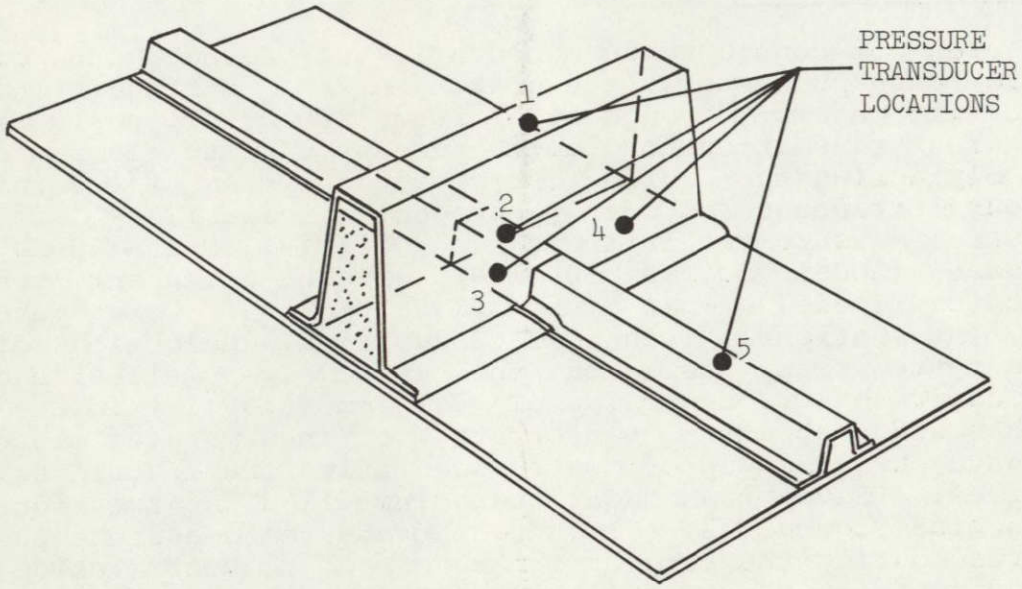

1. BETWEEN FRAME FOAM AND UPPER CAP LAMINATE.
2. BETWEEN STRINGER FOAM AND STRINGER LAMINATE UNDER FRAME FOAM.
3. BETWEEN LOWER CAP LAMINATE AND STRINGER FOAM UNDER FRAME FOAM.
4. BURIED IN LOWER CAP LAMINATE UNDER FRAME FOAM.
5. BURIED IN STRINGER LAMINATE OVER STRINGER FOAM.

FIGURE 13. PRESSURE TRANSDUCER LOCATIONS, PRESSURE TRANSFER TEST.

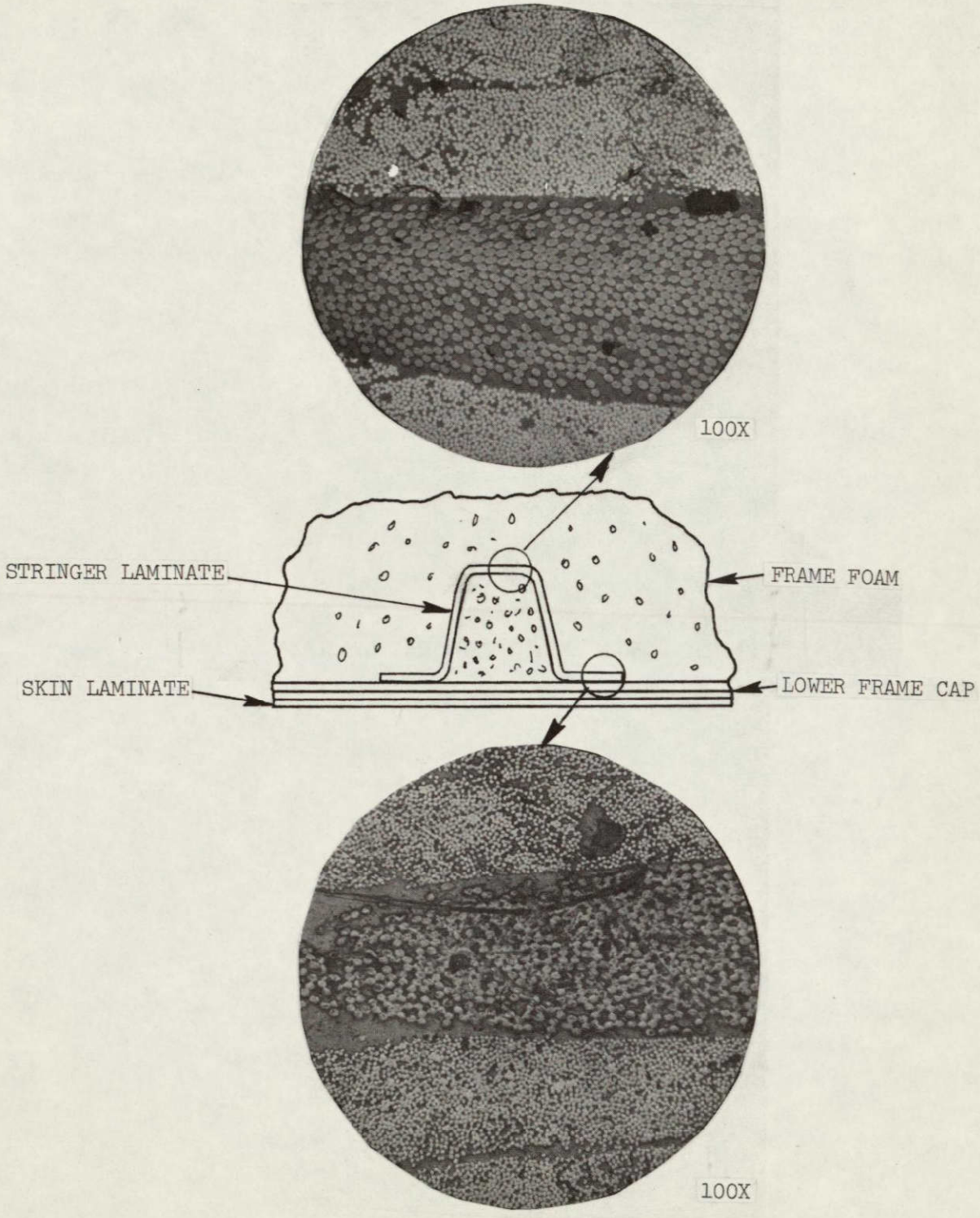

FIGURE 14. PRESSURE TRANSFER THROUGH FOAM IS ADEQUATE TO PRODUCE LOW VOID CONTENT LAMINATE WHERE STRINGER PASSES THROUGH FRAME.

THIS PAGE LEFT INTENTIONALLY BLANK

SECTION 4.0 GENERAL EVALUATION AND SELECTION OF TOOLING

A survey of the major aircraft companies engaged in composite hardware programs was conducted. Six companies were selected as having active program most similar to the program to be conducted at Sikorsky. Arrangements were made to visit with the six companies and discuss with their cognizant people, the rationale for selection of tooling and materials used in these programs. As shown in table VI each of the companies contacted had specific programs directed towards processes with which they were most familiar. All companies expressed a preference for steel tooling for prototype and production fabrication of advanced composite materials. It was generally agreed that nonmetallic, glass/epoxy, tooling would also be a desirable concept, providing the ability to fabricate low cost compound curvature tooling. A major stumbling block to wider acceptance and usage of glass/epoxy tools have been the problems experienced with leakage. At Sikorsky Aircraft, leakage in glass/epoxy tooling has been eliminated through a continuing program of tooling material and process development and control. All tools are stage laminated, or fabricated in multiple steps. In each laminating step a predetermined number and combination of reinforcing ply's are applied to the tool being fabricated. The tool layup is then placed under vacuum and the resin allowed to gel at room temperature. The number of laminating steps employed in the fabrication of any tool depends on the size of the tool. Even the smallest tools are stage laminated in two steps. At present more than 4000 glass/epoxy shell type, high temperature, 176.7°C (350°F) tools have been fabricated for autoclave use.

With the establishment of the one step cure composite frame and stringer reinforced skin as the manufacturing concept, only two candidate tooling approaches were determined as applicable and therefore considered: a female tool constructed to the outside mold line of the aircraft; or a male tool constructed to the inside mold line of the skin, frames, and stringers. Each approach has advantages and disadvantages summarized as follows: In a male tool (Figure 15), recesses are provided for the stringers and frames, producing a precise alignment of these components. The inner surface of the airframe component is the hard tool finish molded surface. The outer or aerodynamic surface of the fabricated component will however, reflect all fabrication discrepancies, tolerance buildups, and material variations. Process cycle times will be extended due to the greater complexity and mass of tooling. A female tool, (Figure 16), produces an airframe component with a finished outer or aerodynamic surface. The complexity of the tool is reduced, therefore tool mass is reduced, permitting faster heat-up rates and reduced cycle time. Placement and maintenance of frame and stringer element location on the tool becomes a major problem. Shifting during cure, and

TABLE VI
INDUSTRY SURVEY OF SUCCESSFUL TOOLING USAGE
FOR ADVANCED COMPOSITES FABRICATION

COMPANY VISITED	PREFERRED MATERIAL FOR MOLDS	ALUMINUM MOLD USAGE	GLASS/EPOXY MOLD USAGE	GRAPHITE/EPOXY MOLD USAGE	KEVLAR/EPOXY MOLD USAGE	CERAMIC MOLD USAGE	REUSEABLE SILICONE VACUUM BAGS	COCURING TECHNIQUE USAGE	SELF CONTAINED TOOLING	CAPTIVE RUBBER TOOLING
Northrup Aircraft Hawthorne Calif.	Steel	Yes Flat & Simple Curvature Use Slip Sheets	Yes Experience Vacuum Leakage In Past	Limited Plan To Evaluate A Mat Prepreg	Limited Experience Shrinkage & Distortion Problems	None	In Use	Prefer To Whenever Possible	Definite Goal	None
Rockwell International, Los Angeles Aircraft Div.	Steel	Yes	Intend To Investigate Experienced Leakage In Past	None	None	None	Plan To Dev. In Future	Whenever Possible	None Feel Current Materials Require Autoclave	None
McDonnell-Douglas Airc. Co., Long Beach California	Steel & Alum.	Yes Including a Female Hat Section Mold	Limited	None	None	None	None	Whenever Possible	Captive Rubber Tooling is Applicable	Yes, Steel Aluminum Technique For A Rudder
General Dynamics, Fort Worth Texas	Steel & Graphite/Epoxy	Yes, Flat & Simple Curvature Use Slip Sheets	Yes 22' Fuselage Mold Fab Some Dimen Problems	CR&D Program For a 20' Fuselage Mold In Progress	None	None	Invest-igating	Whenever Possible	None	Tried, Feel Tooling Too Massive For Large Parts
L.T.V., Dallas Texas	Steel & Glass/Epoxy	Yes, Flat & Simple Curvature	Yes a 9' x 4' Mold Used Successfully	None Feel Glass/Epoxy Adequate	Yes, But Have Experienced Shrinkage & Distortion Problems	None	Invest-igating	Definite Goal	Definite Goal	None
McDonnell Aircraft, St. Louis Missouri	Steel	Yes, On Male Molds Compensate in N.C. Machining For Difference in Thermal Cofff.	None Have Starter Risk Reduction Program To Dev. A 10'L x 4'W	None	None	None	Yes	Definite Goal	Definite Goal	None

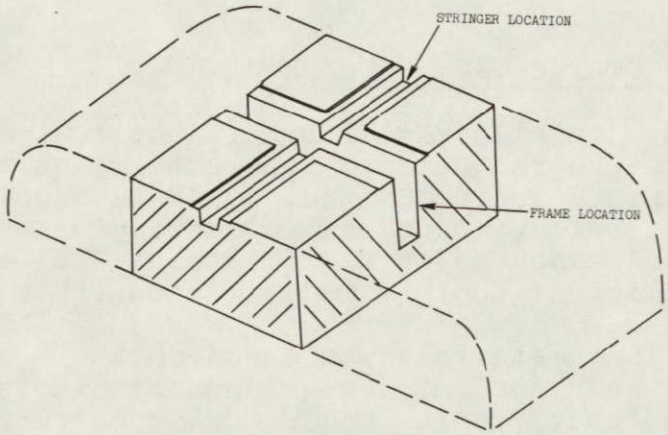

FIGURE 15. MALE TOOL PROVIDES ACCURATE LOCATION OF SHELL ELEMENTS.

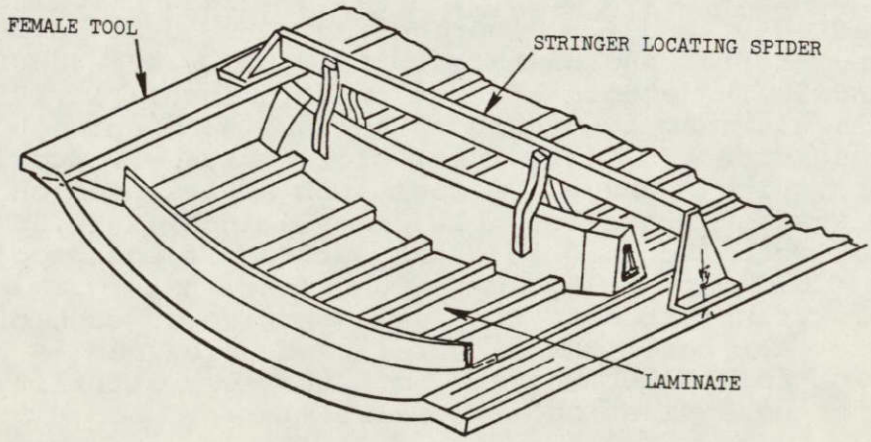

FIGURE 16. FEMALE TOOL ALLOWS EASIER FABRICATION.

misplacement during layup, can cause major repairs or even rejection of large components. To eliminate or minimize mislocation of the structural elements, a locating spider or skeleton frame would have to be developed to act as a positioning jig during layup, and a holding fixture during cure.

4.1 TOOLING FOR STATIC TEST SPECIMENS

The female OML (Outside Mold Line) tooling approach was selected for this program based on the conclusion that solution of the problem areas as recognized, could be accomplished more readily, and the tooling produced would provide the additional advantage of allowing major modifications to the airframe components with minimal tooling modifications.

Selection of tooling materials was based on the results of the industry survey and tooling experience at Sikorsky Aircraft. It was decided that tools would be constructed from two candidate materials: steel plate, and glass/epoxy/honeycomb sandwich. Tool tryout specimens would be fabricated on these tools, and dimensional, thermal, and distortion measurements taken to provide the information for selection of one tool for fabrication of all subsequent test specimens.

The steel tool (Figure 17) consisted of a 71 cm (28 in) square by .64 cm (.25 in) thick steel plate ground flat with a minimum 32 microinch finish on the mold surface.

The glass/epoxy tool (Figure 18) is of sandwich construction consisting of 14 plies of style #7500 glass tooling fabric, alternated @ 0° and 45°, impregnated with U.S. Gypsum #L503 laminating resin and surfaced with U.S. Gypsum #S408 Surface coat, sandwiching a core of 2.54 cm (1.0 inch) X .95 cm (3/8 inch) cell aluminum honeycomb. The core was vented by slitting the surface with .3cm (1/8 inch) slots spaced 3.54cm (1.0 inch) on centers. The honeycomb tool was fabricated on a surface plate to insure flatness. 10.2cm (4 inch) X 10.3cm (4 inch) grid lines were scribed into the surface of both tools to form a 50.8cm (20 inch) X 50.8cm (20 inch) net grid. The grid pattern is transferred to the skin surface of each of the test specimens at cure temperature, and provides a basis of measurement for determination of the compatibility of the tooling to the laminating materials.

Location of the stringer and frame foam core is accomplished by the provision of a steel angle, machined to the same cross section as the foam cores and incorporating a vertical steel slot centered in the face of the angle. The foam cores are manually positioned, visually aligned with the steel locators, and drilled to accept a steel dowel pin, see Figure 19. The slot/pin combination permits only vertical movement of the foam

FIGURE 17. STEEL TOOL USED FOR FABRICATION OF FRAME/STRINGER/SKIN TEST SPECIMENS.

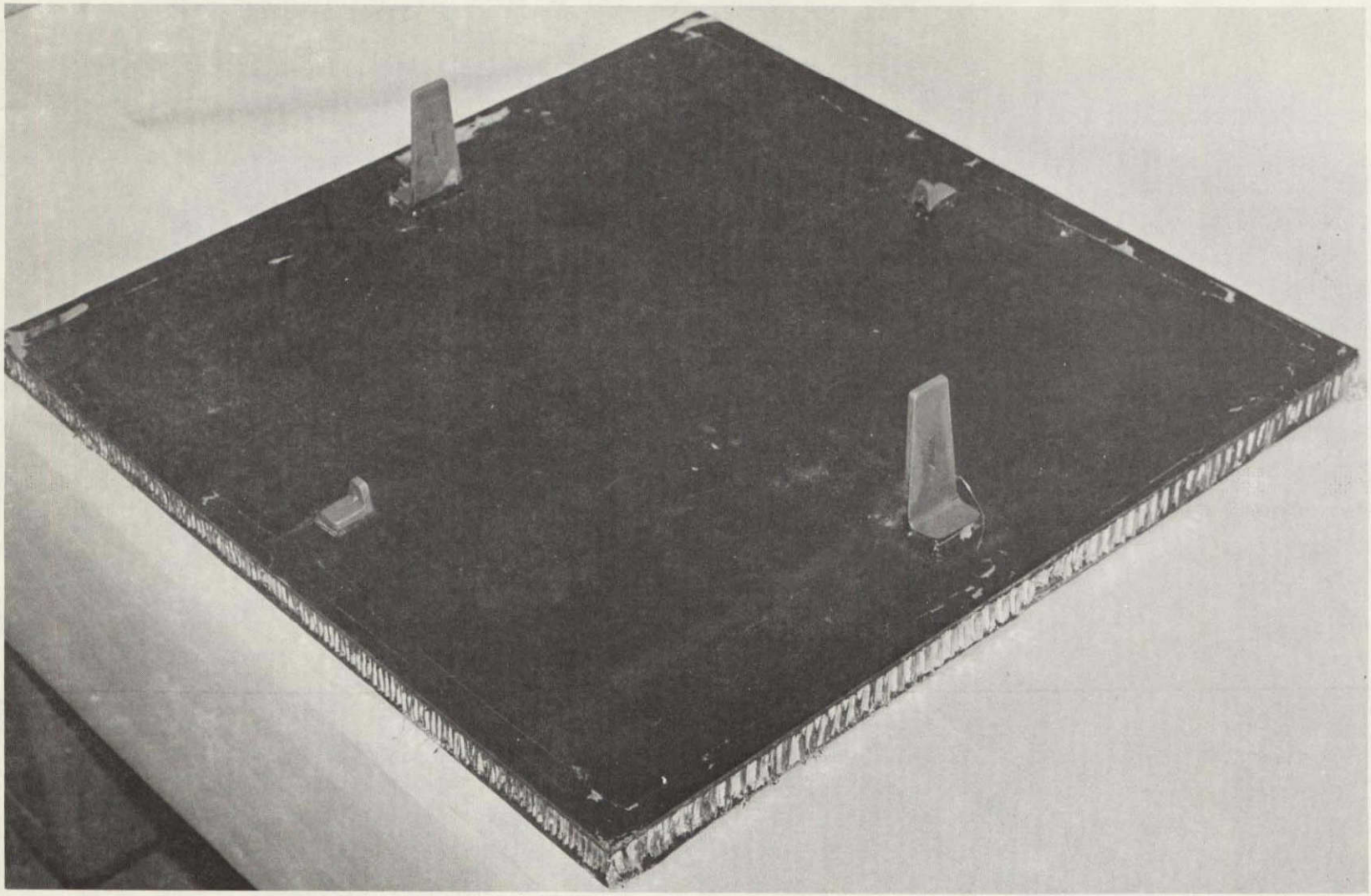

FIGURE 18. GLASS/EPOXY SANDWICH TOOL USED TO EVALUATE ALTERNATE TOOLING CONCEPT.

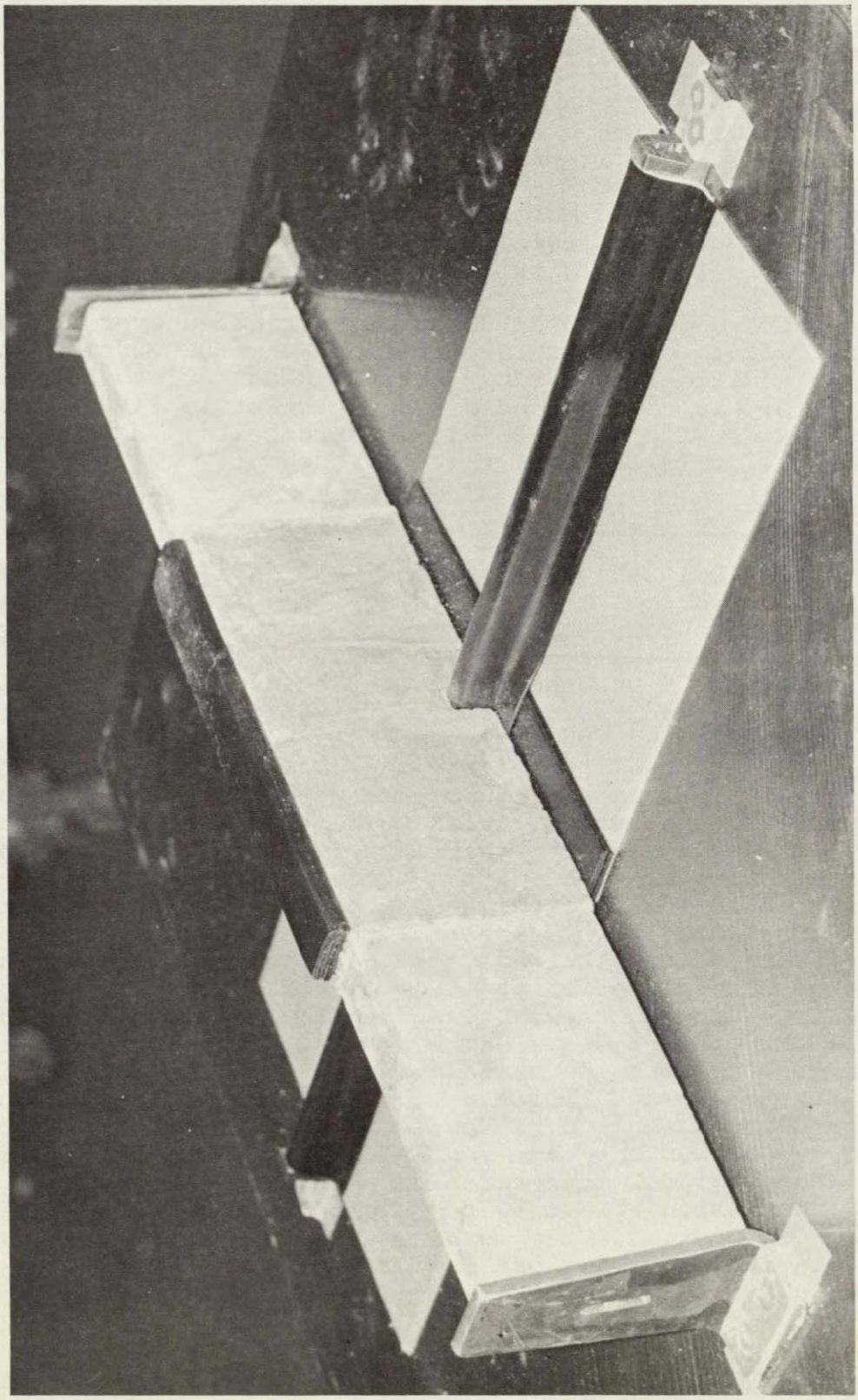

FIGURE 19. PARTIALLY COMPLETED TEST SPECIMEN SHOWING FRAME AND STRINGER FOAM CORES POSITIONED BETWEEN LOCATOR ANGLES.

ORIGINAL PAGE IS
OF POOR QUALITY

core, necessary during the debulking of the laminate and during cure of the composite assembly. Foam casting tools for the stringer and the frame foam details consist of female glass reinforced epoxy tools.

For prototype fabrication of the stringer and frame joint attachment splice cap laminates, male aluminum tools as shown in Figure 20 were fabricated. The open channel configuration, with generous draft angles matching those of the stringer and frame laminates permits the use of aluminum as a tooling material when male tools are utilized.

A molded contour bag (Figure 21) was fabricated over a wood mandrel constructed to the outer surface of the frame and stringer plus additional clearance for a glass cloth bleeder blanket. The bag is constructed of 3 ply of style #1000 glass fabric impregnated with DOW 9705 silicone rubber. The bag is approximately .47cm (3/16 inch) thick throughout.

4.2 TOOL EVALUATION SPECIMENS

The first tooling evaluation specimen was fabricated on the glass/epoxy sandwich tool. Upon bagging the specimen, it was found that the contour bag contained areas of porosity, creating sufficient leakage to render the bag unusable. A repair was effected on the bag consisting of a vacuum impregnation of additional Dow Corning 93072 sealant. Subsequent test of the bag proved it to be vacuum tight and ready for use. On the first specimen cured with the contour bag, a bulge was noticed on the frame web at the juncture of the frame web with the skin. The bulge was apparent on both sides of the frame laminate. Analysis of the bag construction revealed that the combination of the 0° glass reinforcement and the rigid positioning, fixed by the peripheral frame clamp arrangement, prevented any movement of the bag in the area of frame/skin intersection. During the cure cycle, where final debulking and consolidation of the material occurs design pressure is transmitted through the bag to all surfaces exept in the frame/skin interface area. The most direct solution to the problem is to provide a means for movement of the bag in the plane of the skin laminate to assure maintenance of pressure throughout the cure cycle. It was decided to fabricate a second contour bag. In the skin areas, adjacent to the frame and stringer intersection, a series of one or two chevron type expansion pleats were provided. (See Figure 22). As pressure is applied, the expansion pleat is collapsed producing a lateral movement of the bag towards the frame and stringer buildup. Success of this concept at this time has not been fully verified.

Inspection of the specimens fabricated, and each of the candidate tools revealed the following:

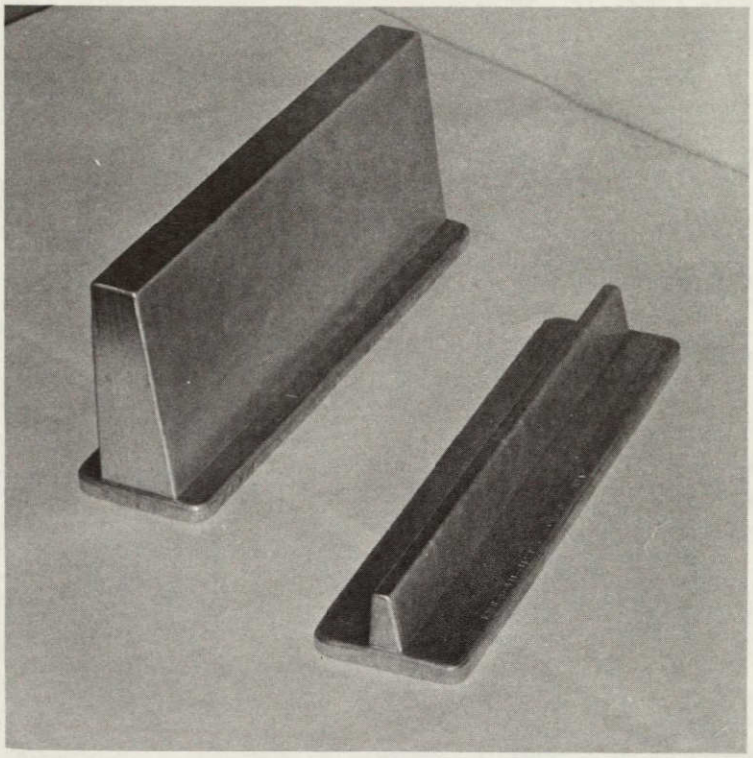

FIGURE 20. MALE ALUMINUM TOOLS ARE SUITABLE FOR FRAME AND STR
SPLICE JOINT LAMINATE FABRICATION.

FIGURE 21. MOLDED CONTOUR BAG IN PLACE ON GLASS/EPOXY HONEYCOMB TOOL.

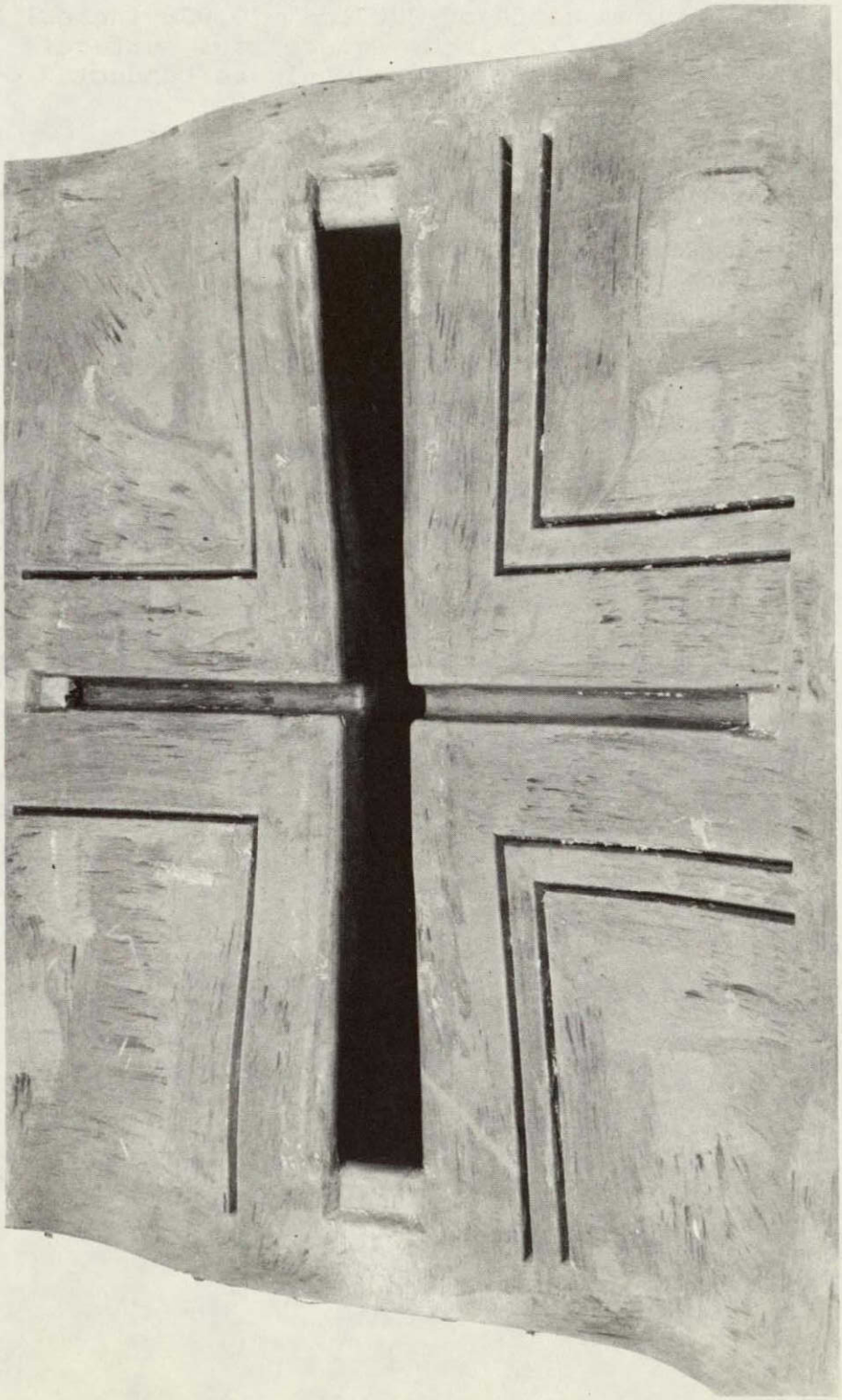

FIGURE 22. MOLDED CONTOUR BAG INCORPORATING CHEVRON TYPE EXPANSION PLEATS.

The surface of the glass/epoxy sandwich tool had become concave, with a maximum depth of 0.071cm (0.028 inches) at the center of the 71.1cm (28 inch) square tool surface. It was decided that no further evaluation would be conducted at this time, with the sandwich tool.

The next two specimens, fabricated in the steel tool were inspected to determine the expansion of the tool at the gel temperature of the composite matrix. Measurement of the 10.2 cm (4 inch) X 10.2cm (4 inch) grid pattern transferred from the tool surface onto the specimen skin surface indicates a growth at temperature of 0.038cm (0.015 inches) in the 50.8cm (20 inch) frame direction and 0.023cm (0.009 inches) in the stringer direction on the full frame specimen. The full stringer specimen verified a tool growth of 0.028cm (0.011 inches) in the stringer direction and .025cm (0.01 inches) in the frame direction. The specimens evaluated for dimensional stability and tool performance were of excellent laminate quality and they were utilized as test specimens. Fabrication details are described in the fabrication section.

In the design of tooling for large airframe components to be fabricated in a female outside mold line tool, consideration must be given to the thermal mismatch between the tool and the composite laminate. Provision for lateral movement in the positioning hardware used to locate the frame and stringer elements must be incorporated into the basic design of each tool. Location of the frames and stringers must be accurately predictable and reproducible from adjacent part to part to minimize misalignment and facilitate attachment.

SECTION 5.0 FABRICATION OF FRAME AND STRINGER TEST SPECIMENS

Sufficient Narmco 5209/T300 Graphite, 15.88kg (35 lbs) and 5209/KEVLAR-49, 4.5 kg (10 lbs) was purchased to fabricate eight EWR 39411 test specimens assembly's consisting of: four stringer test specimens EWR 39411-041 and four frame test specimens EWR 39411-042 four EWR 39411-113 stringer splices and four EWR 39411-114 frame splices. See Figure 3a and 3b for specimen drawing details.

Prior to the fabrication of specimens, process control/sequential ply layup verification check lists were prepared. These sheets are designed to provide layup technicians with sufficient information to cut and prepare material, arrange and layup material in sequential order, and to provide a checklist for verification of ply count during layup. Aluminum sheet patterns were then prepared for each individual size requirement.

Preparation of all specimens followed the same basic procedure. Specific fabrication sequence details shown in Figures 23, 24, 25, 26, 27 relate to the fabrication of the stringer test specimens, but are applicable to the fabrication of all specimens. Specimen preparation consisted of:

1. Preparation of foam details, both foam in place core, and syntactic foam used in the areas of attachment where the core must withstand high compressive loads due to bolted attachments or fittings.
2. Cutting of graphite/KEVLAR preimpregnated materials to the patterns and in the required numbers and orientation defined in the process control layup sheets.
3. Pre-fabrication, layup of all 0° oriented materials. (Upper and lower frame caps and stringer web.)
4. Layout of patterned materials in sequential order for layup.
5. Layup of materials on tool in accordance with sequential process control sheets.
6. Bagging with molded pre-formed silicone rubber contour bag.
7. Cure in autoclave at temperature and pressure as developed during the materials evaluation portion of the program.

5.1 FOAM FABRICATION

The rigid 221Mg/m^3 (8 lb/cu ft) density polyurethane foam EWR 39411-101 and -102 cores (Stathane 8747) were prepared by casting into release coated female epoxy molds fabricated to the finished shape of the required stringer or frame core. Because of the extremely small amounts of foam required to charge each tool cavity, automatic foam casting machinery was not utilized. Manual individual batch proportioning, mixing and pouring was used for casting each foam core. As expected, with batch mixing and dispensing, there was a large variation

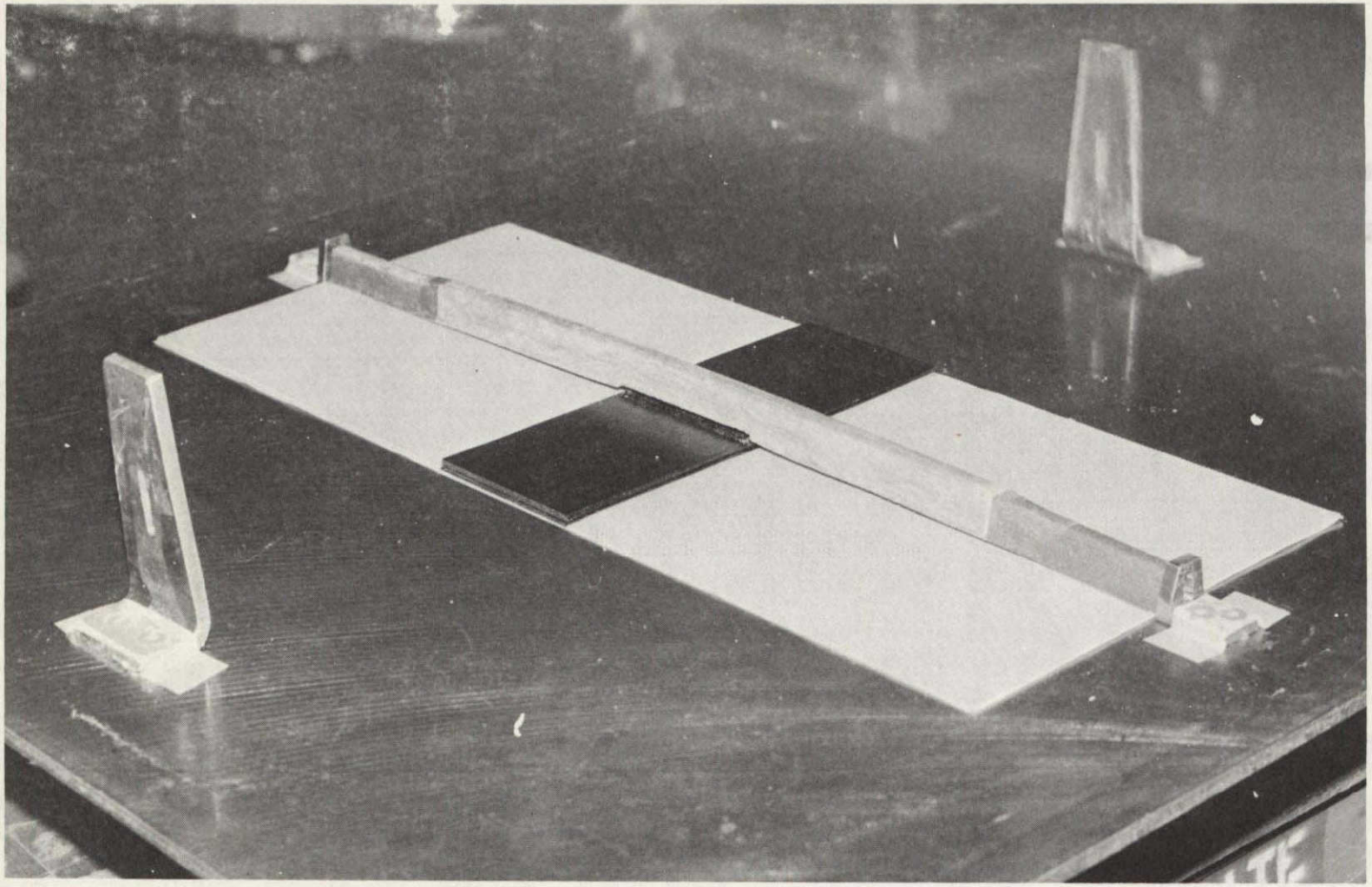

FIGURE 23. LAYUP OF EWR-39411-041 STRINGER TEST SPECIMEN SHOWING SKIN LAMINATE, LOWER CAP LAMINATE, AND STRINGER FOAM IN PLACE ON STEEL TOOL.

ORIGINAL PAGE IS
OF POOR QUALITY

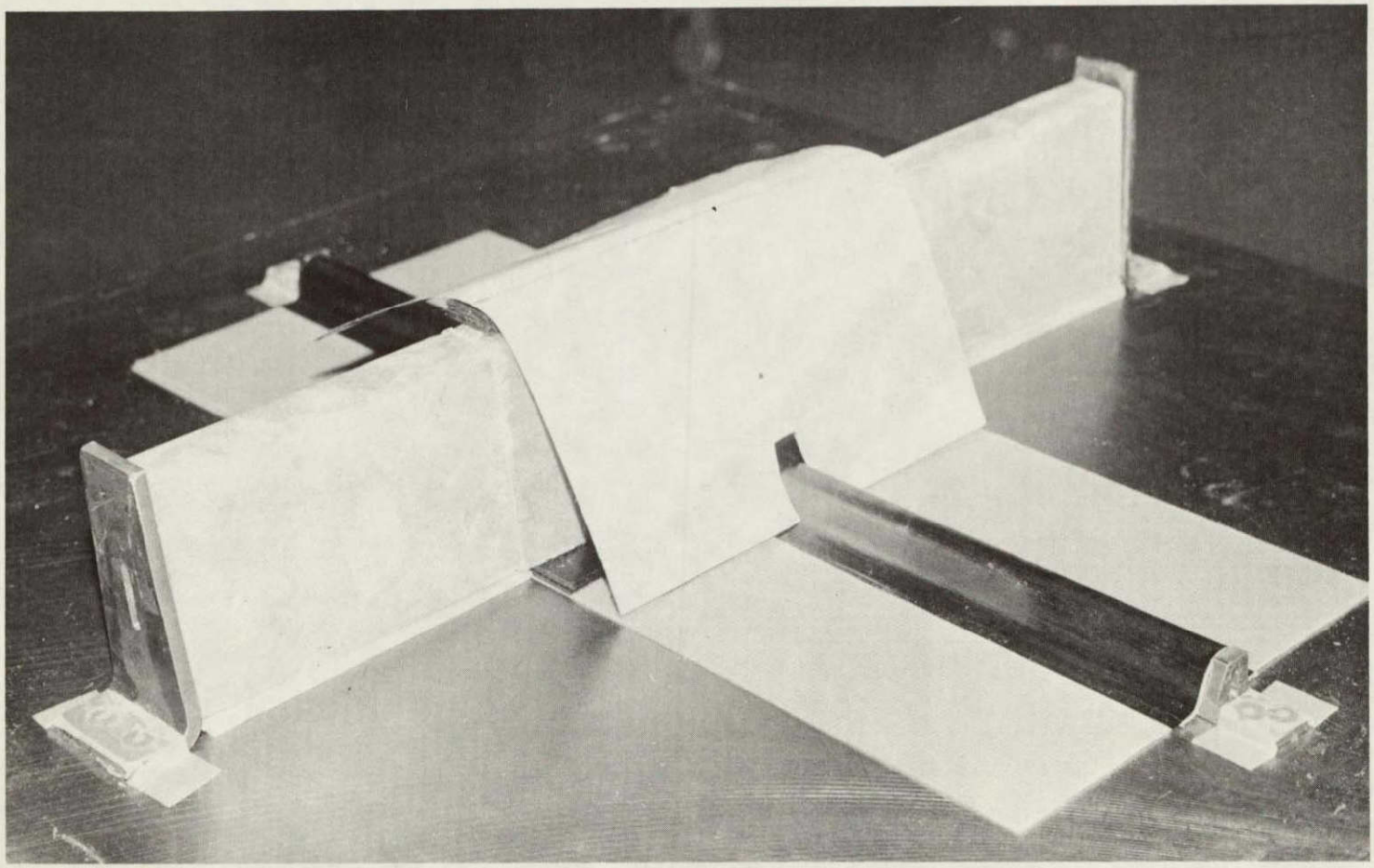

FIGURE 24. LAYUP OF EWR-39411-041 STRINGER TEST SPECIMEN SHOWING STRINGER LAYUP COMPLETED, FRAME FOAM IN PLACE, AND FIRST PLY OF FRAME REINFORCEMENT IN POSITION.

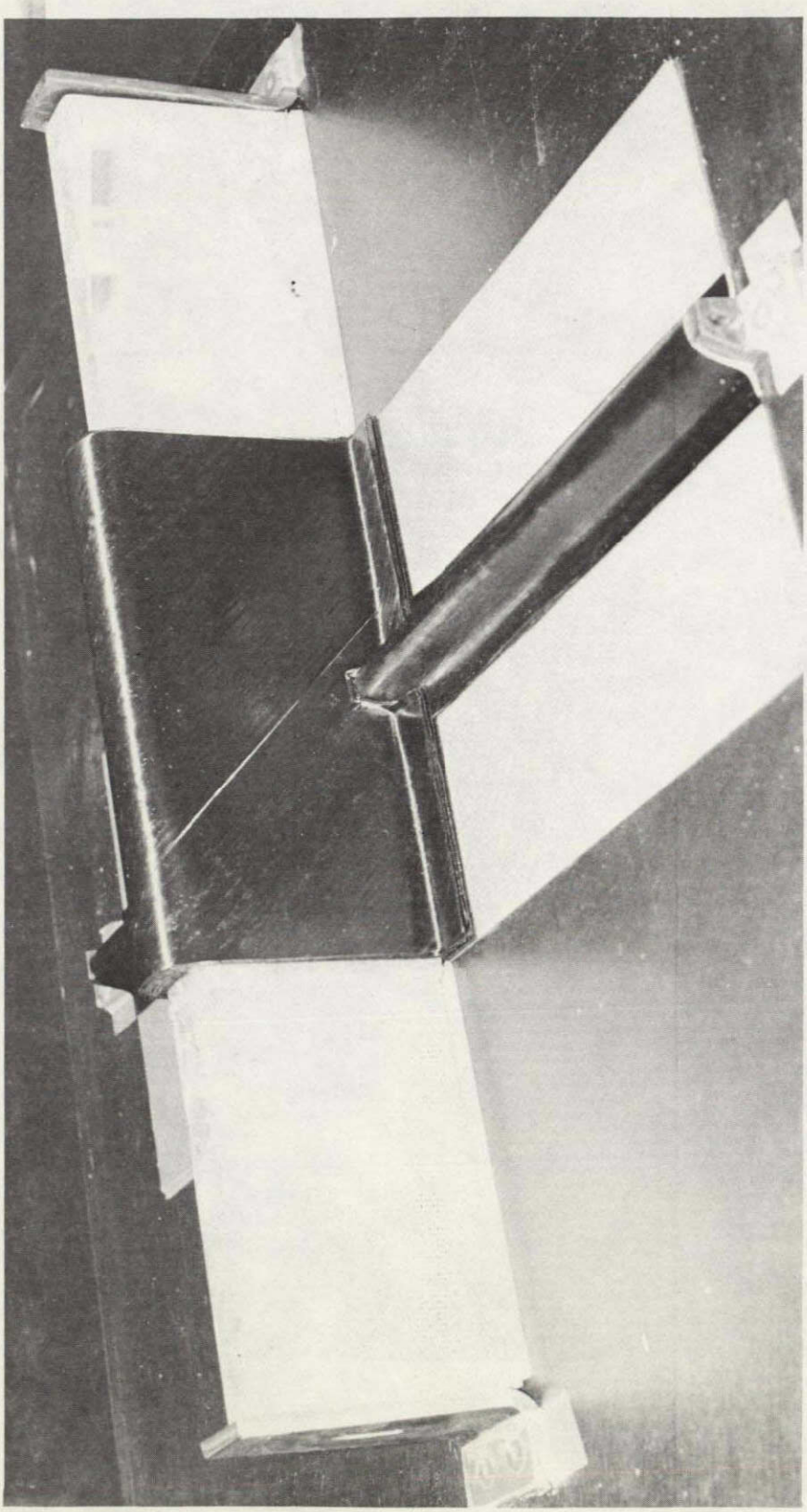

FIGURE 25. LAYUP OF EWR-39411-041 STRINGER TEST SPECIMEN SHOWING LAYUP COMPLETED.

ORIGINAL PAGE IS
OF POOR QUALITY

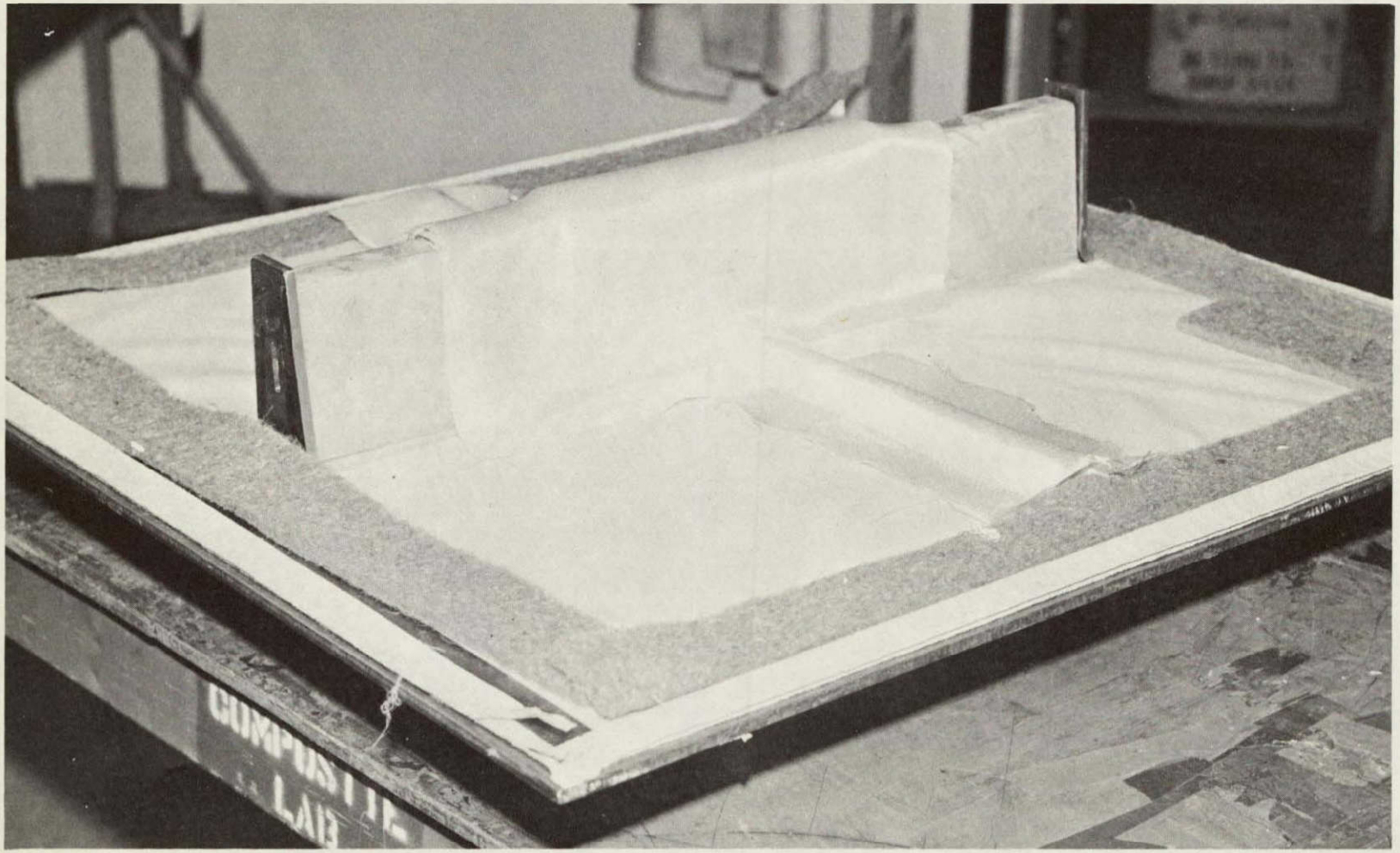

FIGURE 26. LAYUP OF EWR -39411-041 STRINGER TEST SPECIMEN WITH BLEEDER PLIES IN POSITION.

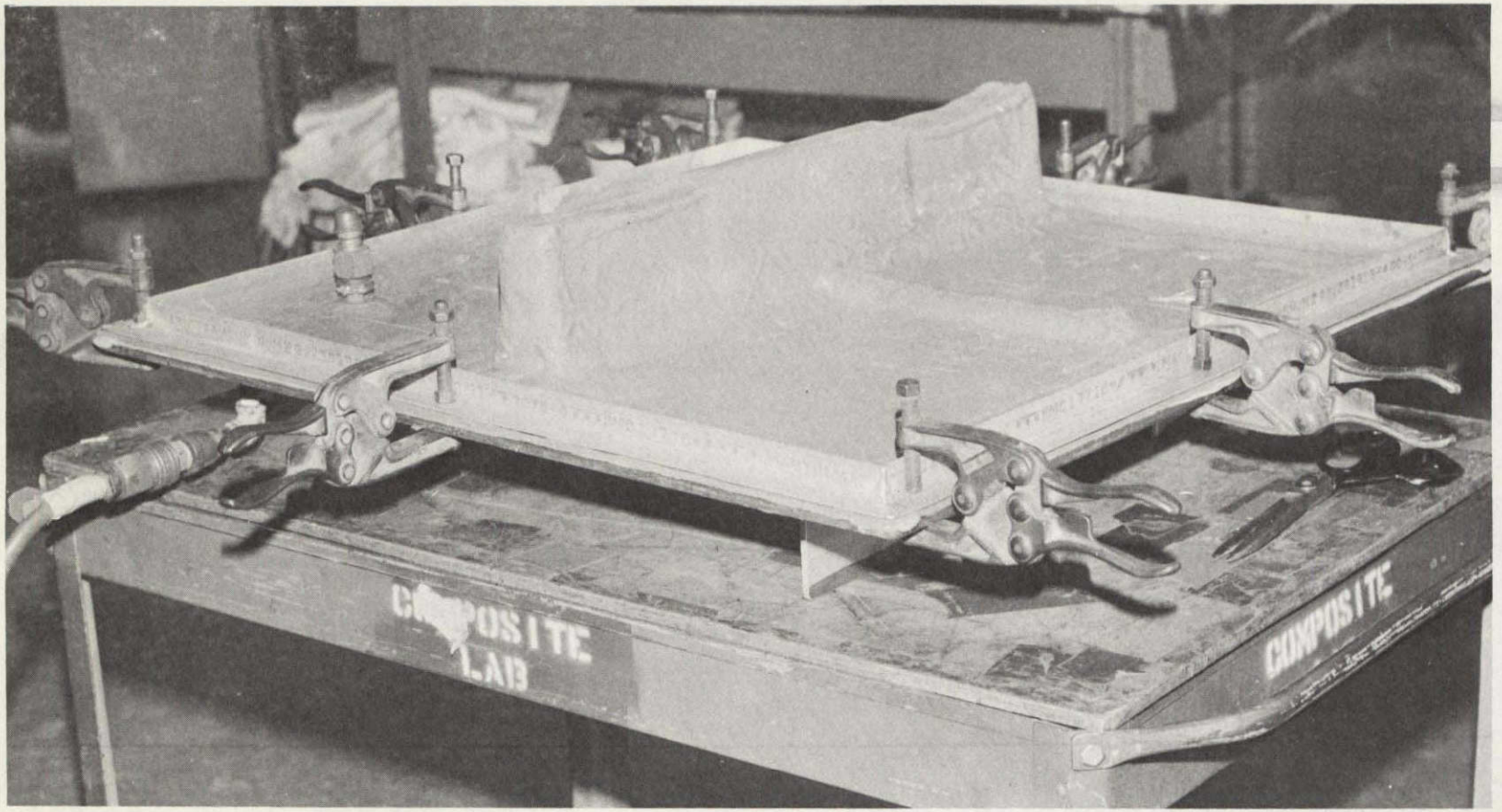

FIGURE 27. EWR-39411-041 STRINGER TEST SPECIMEN LAYUP UNDER VACUUM IN PERMANENT ELASTOMERIC BAG.

in the density of similar cast foam details. This large variation in foam densities was to have a bearing in the successful fabrication of both the stringer and the frame test specimens.

5.2 SPECIMEN FABRICATION

Fabrication of specimen #1 varied from the above established procedure because of a delay in the completion of the silicone rubber bag. Specimen #1 was vacuum bagged utilizing a conventional nylon film bag secured to the tool surface with a high temperature vacuum bag sealant tape. Inspection of the cured EWR 39411-042, #1 specimen provided the following information; adequate compaction was achieved in all exposed laminates as shown in Figure 28a. Compaction of the lower cap was also adequate, indicating a uniform pressure transfer through the -101 frame foam. A small amount of the 0° graphite from the upper cap was extruded into the web at the upper sides of the frame. Similarly a small amount of the 0° graphite from the lower cap was extruded into the skin/web flange intersection. Laminate definition in the areas of the frame/skin and stringer skin was irregular. All of the conditions exhibited in the first specimen were attributed to the absence of a contoured premolded vacuum bag to provide the support and definition necessary to produce a uniform cross-sectioned part.

For fabrication of specimen #2 the contour premolded silicone rubber bag was available. Layup of the EWR 39411-042 #2 specimen proceeded according to schedule. During the layup a number of innovative procedures were incorporated into the layup sequence to simplify or eliminate some of the procedural bottlenecks encountered during the layup of specimen #1. The frame web, and frame joint reinforcement plies were pre-plied into pairs, ie: 0°, 90° and +45°, -45°. Incorporation of this seemingly insignificant step produced a threefold advantage:

1. It stabilized the plies of unsupported graphite during application and subsequent removal of carrier paper.
2. It prevented the distortion or wandering of off axis ($\pm$45°) plies as previously encountered, when individual plies were wrapped onto the frame foam form.
3. It reduced by 1/2 the number of labor hours required to form the required number of plies to the shape of the frame.

Another extremely effective step involved the use of teflon "slip-sheets". The layup procedure as developed required that each web ply be positioned with its center line coinciding with a center line locator marked at the ends of the frame foam. After location, each ply was worked into place to conform to the frame cross section shape. As the graphite prepreg being mechanically worked into the frame web, contacted the KEVLAR skin laminate, the tack of the two materials caused immediate

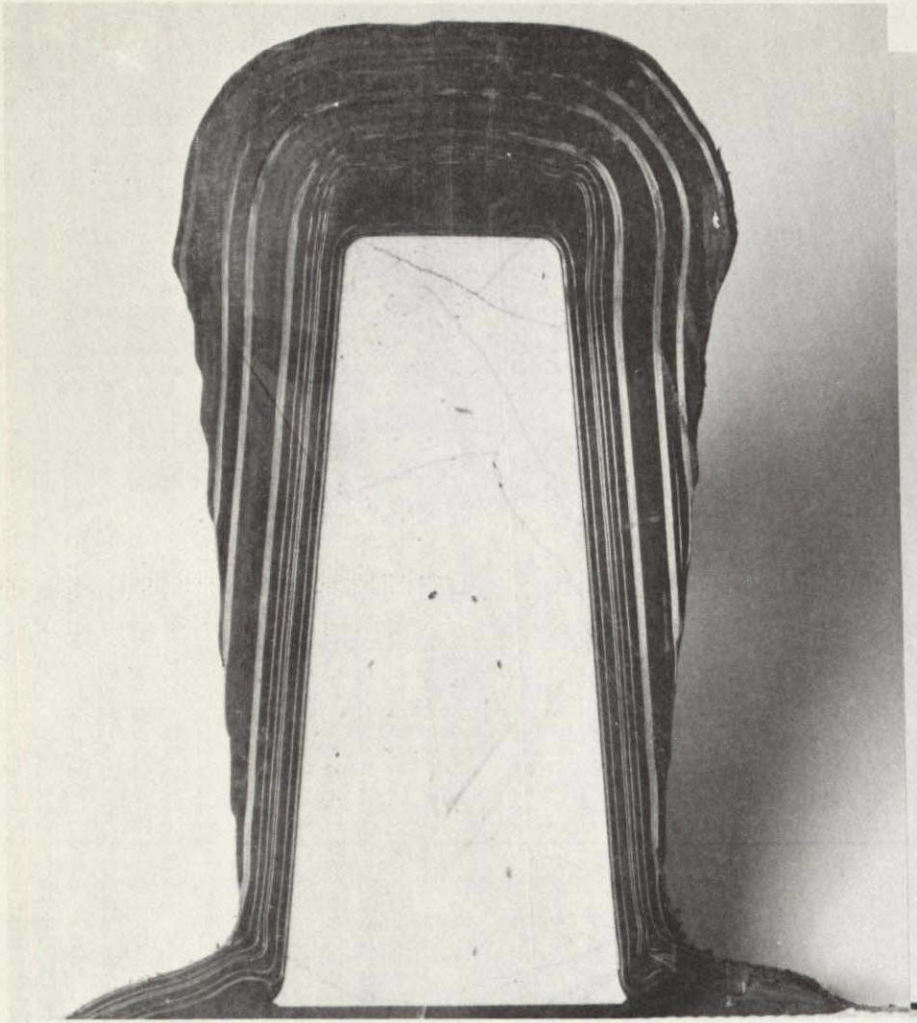

FIGURE 28a. CROSS SECTION VIEW OF FRAME LAMINATE EWR-39411-042 SPECIMEN #1 (WITH LAMINATED FRAME BENDING DOUBLERS IN PLACE).

FIGURE 28b. CROSS SECTION VIEW OF FRAME LAMINATE EWR-39411-042 SPECIMEN #2 SHOWING WEB LAMINATE BULGES AT BASE OF FOAM.

adhesion, preventing the graphite from being sufficiently compacted to produce a well defined frame/skin intersection. Placement of a teflon "slip-sheet" on the skin surface extending to the frame/skin intersection, prior to the application of each ply of graphite prepreg, facilitated the compaction of that ply. After compaction of the ply to, and including the skin/frame intersection, the "slip-sheet" was removed and the flange laminate compacted. Upon completion of the layup, the contour bag was positioned and vacuum drawn. The contour bag was found to have a number of leaks or porous areas, and therefore was not useable. As in specimen #1 a conventional film bag was used. Inspection of EWR 39411-042 #2 specimen revealed a specimen essentially the same as specimen #1 with one exception; a marked improvement in the definition and compaction of the laminate in the frame/skin intersection area. EWR 39411-042 Stringer Specimen #3 was fabricated using the exact procedures described for specimen #2. The silicone contour bag had been sealed and was used for vacuum bagging of the #3 specimen. Upon inspection of the #3 specimen, two significant differences were immediately apparent.

1. The contour and definition of the laminates in both the frame and stringer were much improved as shown in Figure 28b. There was better containment of the 0° cap laminate and an even greater uniformity at the skin/stringer juncture.
2. Also shown in Figure 28b large bulges signifying areas of poor compaction due to low pressure occurred at the base of the frame laminate, on both sides.

It is believed that the silicone contour bag, molded to the uncompacted ply thickness of the graphite laminate, reinforced with a square weave glass fabric, and rigidly fixed about its periphery by means of a frame and clamps was unable to move at the base of the frame when pressure was applied, thus creating the resulting bulges. It was decided at this time to continue fabrication of the remaining specimens using conventional bagging techniques, and to attempt, within the time frame available, the fabrication of a new contour bag incorporating expansion pleats in the skin plane surface of the bag adjacent to the frame flange areas. The existing contour bag would only be used for cold compaction of the completed layups. Specimens #4, #5, and #6 (EWR 39411-041) were all fabricated with no problems encountered during fabrication and no differences observed when inspected. On EWR 39411-042 #7 specimen some distortion of the -101 frame foam was observed during inspection of the completed laminate. A check of the fabricated weight shows the -101 frame foam used in the fabrication of specimen #7 was of a lower density than any previously incorporated into a test specimen. At this time no further significance was attached to the variation, and the specimen was approved for use as an EWR 39411-042 Frame Splice Joint Test Specimen. Each of the specimens, numbers 4 thru 7

were fabricated using the original silicone contour bag for cold compaction and debulking. When the bag was removed, each of the specimens had developed the bulges at the base of the frame laminate, proving the assumption that the bulges were caused by failure of the bag to provide pressure in that area. The bulge was removed when each of the specimens was rebagged with a conventional nylon film bag before cure.

Specimen #8 (EWR 39411-041) was fabricated with a conventional film bag. Inspection after cure revealed a complete collapse of the stringer foam, and a partial collapse of the frame foam. Upon checking the foam fabrication records it was apparent that both the -101 frame foam and the -102 stringer foam were below the 221Mg/m^3 (8 lb/cu ft) chosen density.

The last specimen was refabricated using foam details manufactured from a new batch of material. The part was then placed under vacuum in the original contour bag for debulking while the new contour bag incorporating the expansion pleats was being fabricated. A decision was made to hold the last specimen under vacuum until the new contour bag was available. Unfortunately by the time the new contour bag was ready, six days had elapsed and the bulges had become so pronounced that they could not be mechanically removed. The part was cured using the new contour bag with expansion pleats. Although the bulges were not completely removed, the expansion pleats provided enough movement to significantly reduce them. It is believed that if this bag had been available for the debulking and the cure of the specimen, the problem of low pressure at the base of the frame laminate would have been eliminated.

To prepare the specimens for test, additional fabrication operations were necessary. The frame bending specimens (-043 Figure 3a) required the application of massive graphite doublers to each end of the specimen to induce fracture in the area of the frame/stringer intersection. Fabrication of the built up non-aircraft attachment doublers was conducted in two operations. As shown in Figures 28a and 29, 92 plies of alternately oriented 0°, 90° and ±45° graphite were cut into patterns, laid up on the specimen frame web, vacuum bagged, and cured in place. In a second operation, precured 92 ply flat laminates were bonded to the skin surface of the specimen. The upper surfaces of the non-aircraft doublers were then machined flat to facilitate positioning in the test fixture.

For the stringer test specimen (-041 Figure 3a), stabilization of the compression ends was required to provide a uniform load distribution over the entire compression surface. The stringer moment of inertia was calculated and a rectangular block of high compression epoxy casting compound was cast on both ends of the specimen as shown in Figure 30. The ends of the cast compression blocks were then machined perpendicular to the

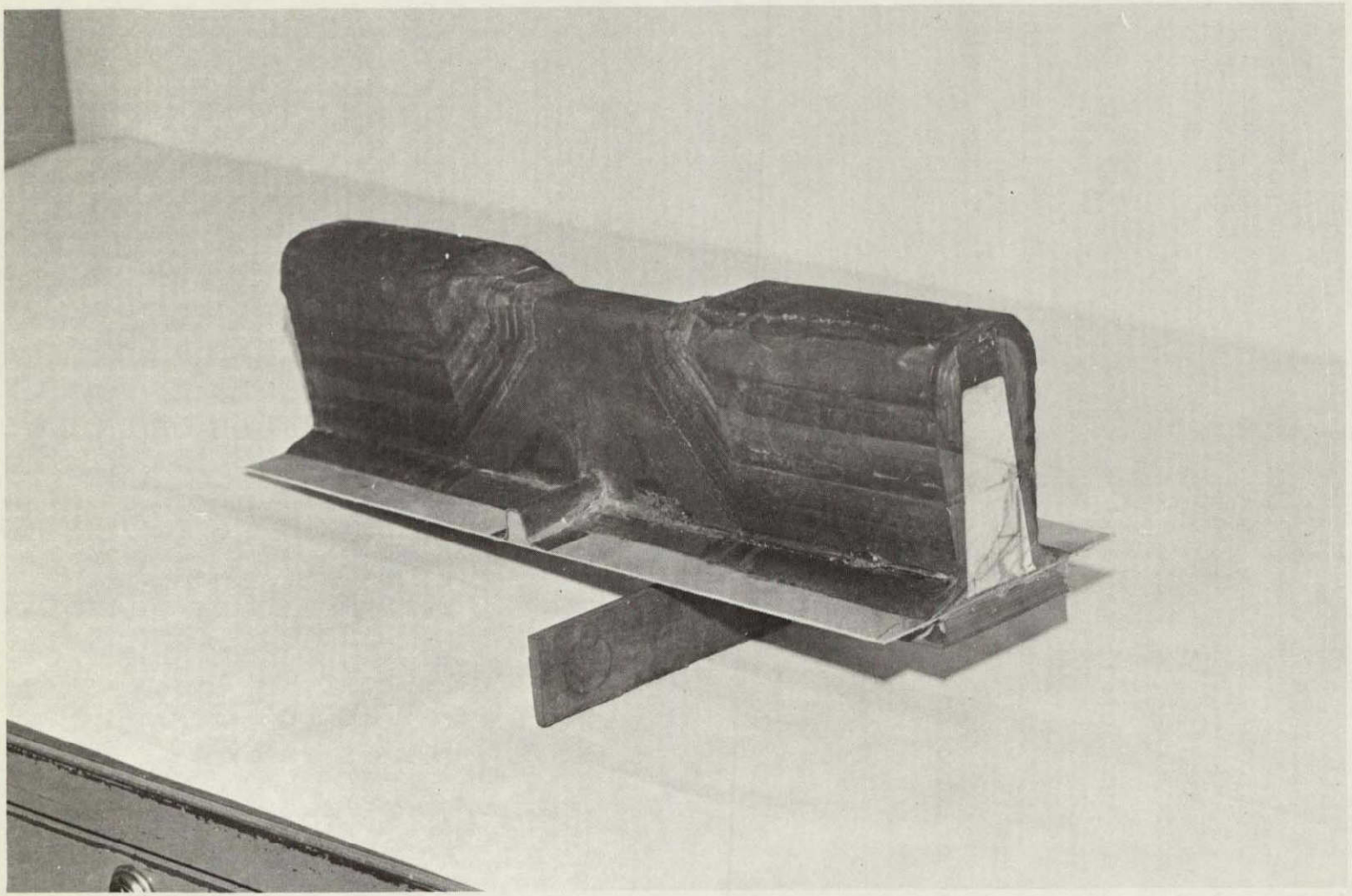

FIGURE 29. FRAME BENDING TEST SPECIMEN REQUIRES MASSIVE LAMINATE BUILDUP TO INSURE FAILURE IN TEST SECTION.

stringer and parallel to within .005 cm (.002 in) to preclude the introduction of any bending moment during the compression test. In a similar operation, each splice cap (-114, Figure 3b) was positioned in a 7.62 cm (3.0 in) diameter tube centered about the centroid of mass of the stringer, and potted with high compression epoxy casting compound as shown in Figure 40. Preparation of the frame splice attachment specimens (-042 Figure 3a) consisted of the mechanical attachment of the (-113 Figure 3a) splice caps to the ends of the specimen.

All required machining operations were performed on the specimens utilizing conventional equipment and techniques. The only special tools required were cobalt steel drills. All holes were first pilot drilled and then final drilled to required diameters. All laminates were back supported with wood or aluminum blocks to prevent fiber damage at the exit face of the drilled hole.

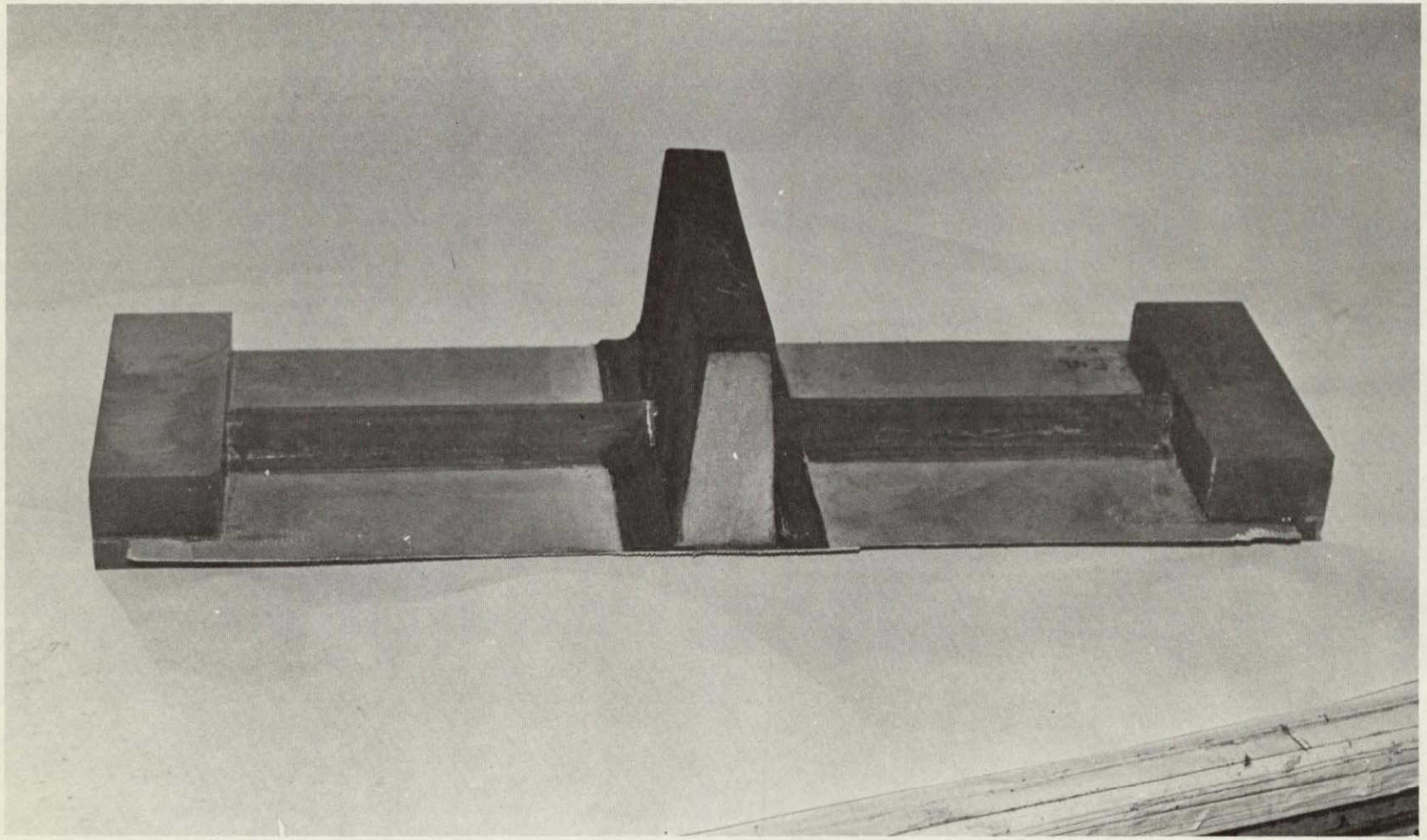

FIGURE 30. FILLED EPOXY POTTED ENDS STABILIZE EWR-39411-041 STRINGER COMPRESSION SPECIMEN.

THIS PAGE LEFT INTENTIONALLY BLANK

SECTION 6.0 STATIC TESTS OF FRAMES AND STRINGERS

6.1 TEST PROCEDURES

The tests conducted in Phase I of this program were designed to substantiate the strength and stability characteristics of the frame and stringer elements under static axial and bending loads. The stringer, and stringer splice, test elements were tested in axial compression and the frame and frame splice were tested in a combination of bending and axial compression. All specimens were loaded to fracture. All specimens were instrumented with bonded electrical resistance strain gages. Locations for strain gage placement were calculated areas of maximum stress and probable failure.

Frame and Frame Splice Attachment Tests

Special test fixtures, as shown in Figure 31 and 32 were designed to test the frame bending, and frame splice joint bending specimens. Application of load to these specimens was through a hydraulic cylinder, coupled to a calibrated load cell. The cylinder was located 5.24 cm (6.0 in) from the neutral axis of the frame to produce the calculated 6 to 1 ratio of bending load to axial compression load. For each test a dial gage was installed to measure normal deflection along the longitudinal center line of each panel with respect to the support structure. Strain measurements were recorded by direct readout from a multi- channel digital strain indicator. The frame splice joint specimen was attached to the test fixture by means of short bolts through each leg of the splice channel laminate. Bolt locations were as required for an aircraft type attachment.

Stringer and Stringer Splice Attachment Tests

The stringer and stringer splice specimens were tested in pure compression in a Baldwin Universal static test machine. Loads were applied incrementally to all specimens, strain and deflection were recorded at each increment and physical characteristics were monitored to determine visual changes.

6.2 TEST RESULTS

The results of all tests are summarized in Table VII.

Frame Bending Specimen Tests

The load schedule for frame bending specimen #1 included two incremental loadings to the design limit load of the frame 49.4 kN (11,100 lb) in steps of 9.79 kN (2,200 lb) and a final loading to fracture. No abnormalities were observed during the two loadings to limit load. During the third loading increment

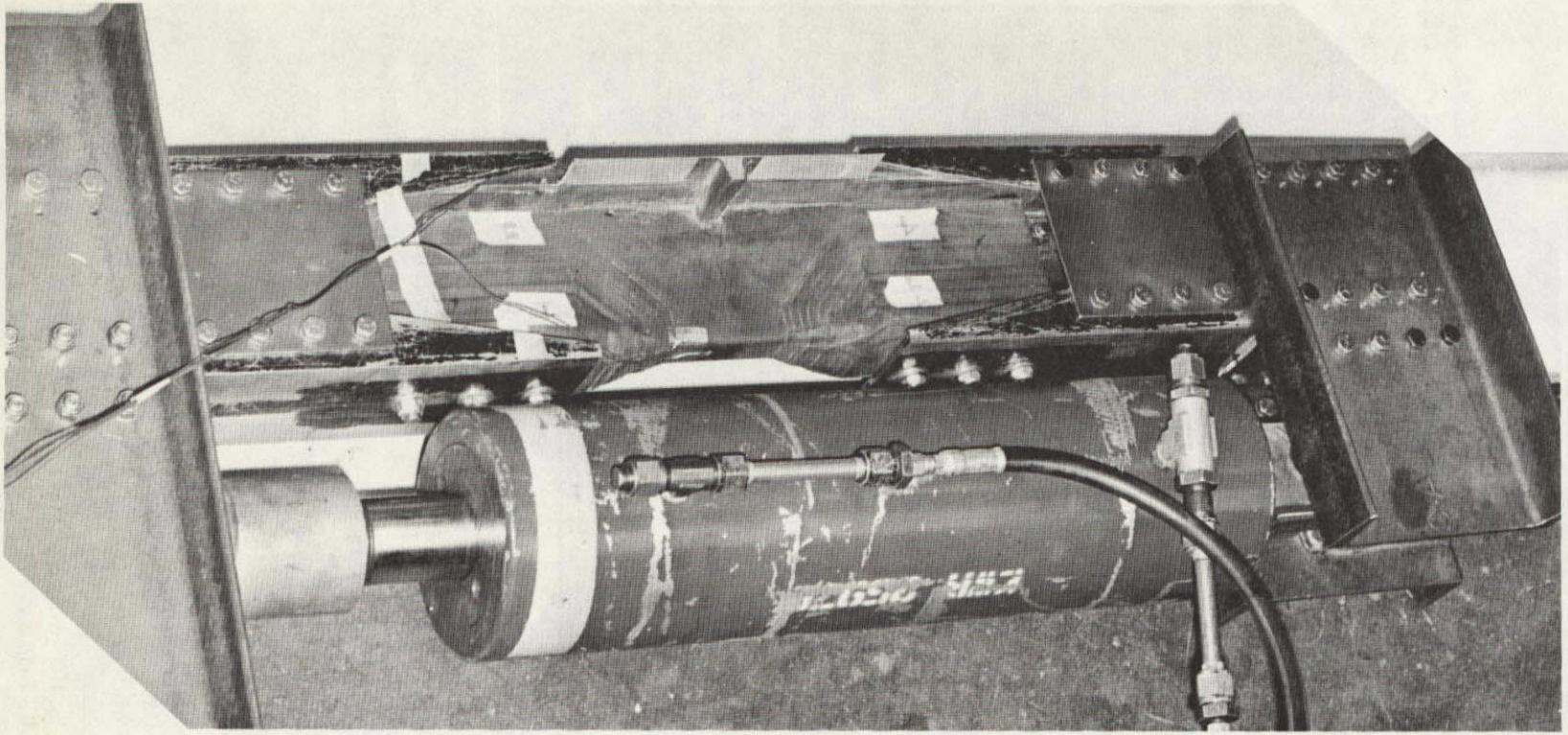

FIGURE 31. FRAME BENDING SPECIMEN INSTALLED IN TEST FIXTURE, SHOWING METHOD OF FASTENING TO FIXTURE AND LOCATION OF HYDRAULIC CYLINDER AND LOAD CELL.

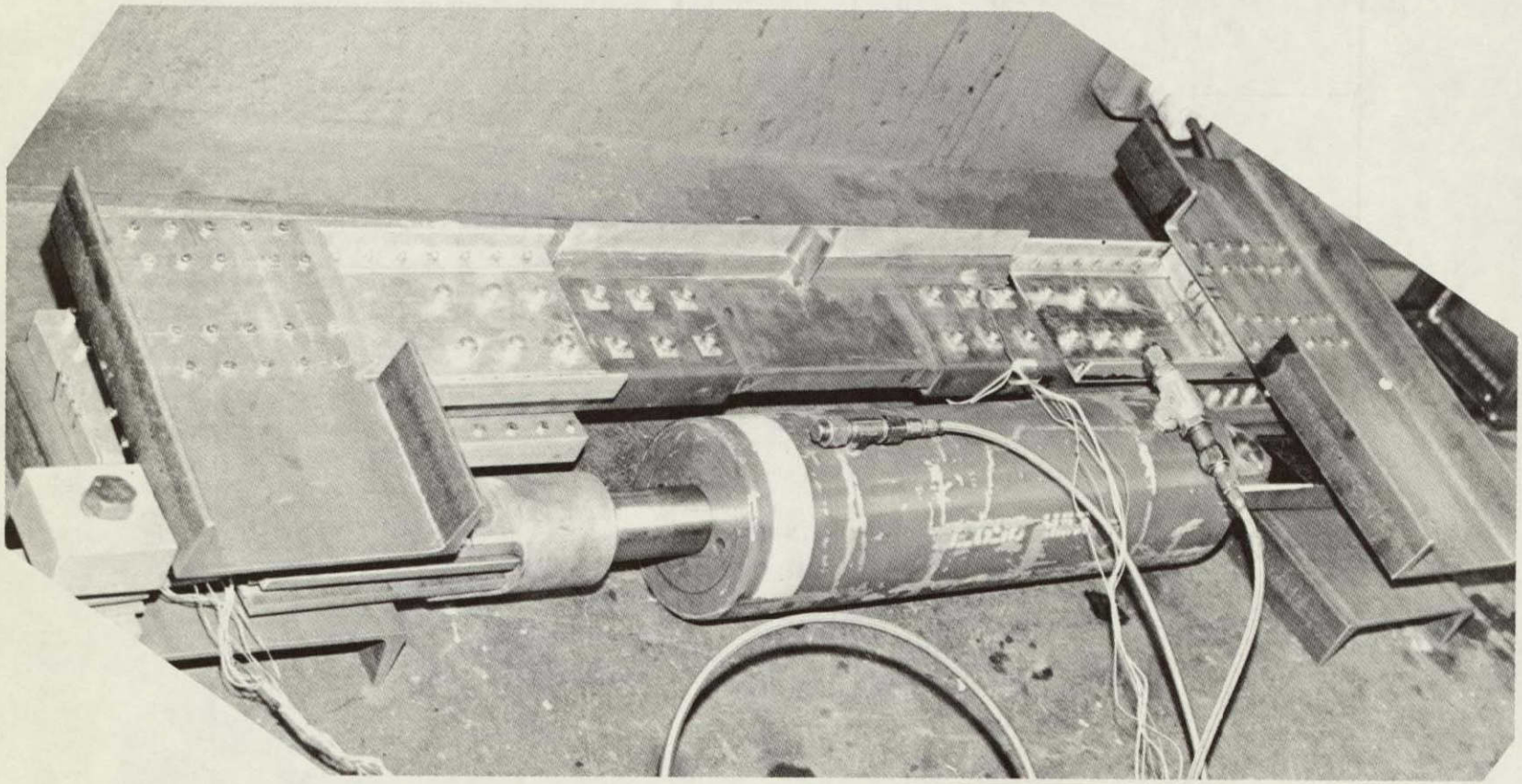

FIGURE 32. FRAME SPLICE JOINT BENDING SPECIMEN INSTALLED IN TEST FIXTURE SHOWING METHOD OF FASTENING TO FIXTURE AND LOCATION OF HYDRAULIC CYLINDER AND LOAD CELL.

TABLE VII

SUMMARY OF TEST RESULTS

TYPE OF SPECIMEN STATIC TEST	ACTUAL FAILING LOAD			
	SPECIMEN #	COMPRESSION NEWTONS (LB)	BENDING MOMENT NEWTON·METER (IN.- LB.)	MAX STRAIN (IN./IN.)
STRINGER-COMPRESSION	1	29 801 (6,700)	-	(5,800)
	2	28 407 (6,400)	-	(4,000)
STRINGER SPLICE COMPRESSION	1	15 568 (3,500)	-	(6,300)
	2	14 678 (3,300)	-	(9,500)
FRAME-AXIAL COMPRESSION & BENDING	1	59 158 (13,300)	10 161 (90,000)	(8,800)
	2	76 061 (17,100)	11 967 (106,000)	(6,500)
FRAME SPLICE AXIAL COMPRESSION & BENDING	1	33 804 (7,500)	5 193 (46,000)	(8,500)
	2	37 674 (8,470)	5 976 (52,940)	(6,300)

an audible indication of failure was heard at approximately 53.4 kN (12,000 lb) load 5000 μ inch/inch strain. The final load at fracture was 76.0 kN (17,000 lb) axial, with a bending moment of 11.98 kN·m (106,900 in lb). Both frame bending specimens failed in compression at the upper frame cap (away from the skin surface), see Figures 33 and 34 and when sectioned, both specimens revealed similar fractures as shown in Figure 35.

Frame Splice Bending Specimen Tests

Both frame splice specimens were loaded to fracture. As shown in Figure 32 the load was applied similarily to the frame bending specimens. Specimen number one fractured at a compressive load of 33.8 kN (7,600 lb) and a bending moment of 5.2 kJ (46,000 in lb). Specimen number two failed at a compressive load of 37.7 kN (8470 lb) and a bending moment of 6.0kN·m52,900 in-lb). The strain at failure was 6300 μ inches/inch for both specimens. As shown in Figures 36 and 37 both specimens fractured identically at the point of maximum stress, in the test fixture. Both fractures originated at or adjacent to the lower bolt hole. As experienced in the testing of the frame bending specimens, numerous audible indications of damage were apparent until fracture.

Stringer Compression Specimen Tests

The stringer specimens were loaded in compression as shown in Figure 38. Fracture occurred at loads of 29.8 kN (6700 lb) and 28.4 kN (6400 lb). Initial failure occurred when the skin laminate separated from the stringer flange laminate. As evidenced in Figure 39a for specimen number one and Figure 39b for specimen number two separation of the skin to stringer flange occurred at the intersection of the densified attachment area and the foam stringer core material. The concentrated load in this area caused the skin delamination. With the loss of the skin due to delamination the stringer laminate fractured in pure compression. The potted ends stabilized the specimens in the test machine and prevented any buckling failure.

Stringer Splice Compression Specimen Tests

The stringer splice specimens were loaded in compression as shown in Figure 40. Specimen number one failed at 15.5 kN (3500 lb). The strain at fracture was 6300 μ inches/inch.

Failure originated in the material between the bolt attachment holes and then continued to the machined edge of the splice cap. See Figure 41a. At no time during the load application was there any indication of failure, visual or audible. Although testing was discontinued at the inception of the original failure to prevent possible conflicting multiple

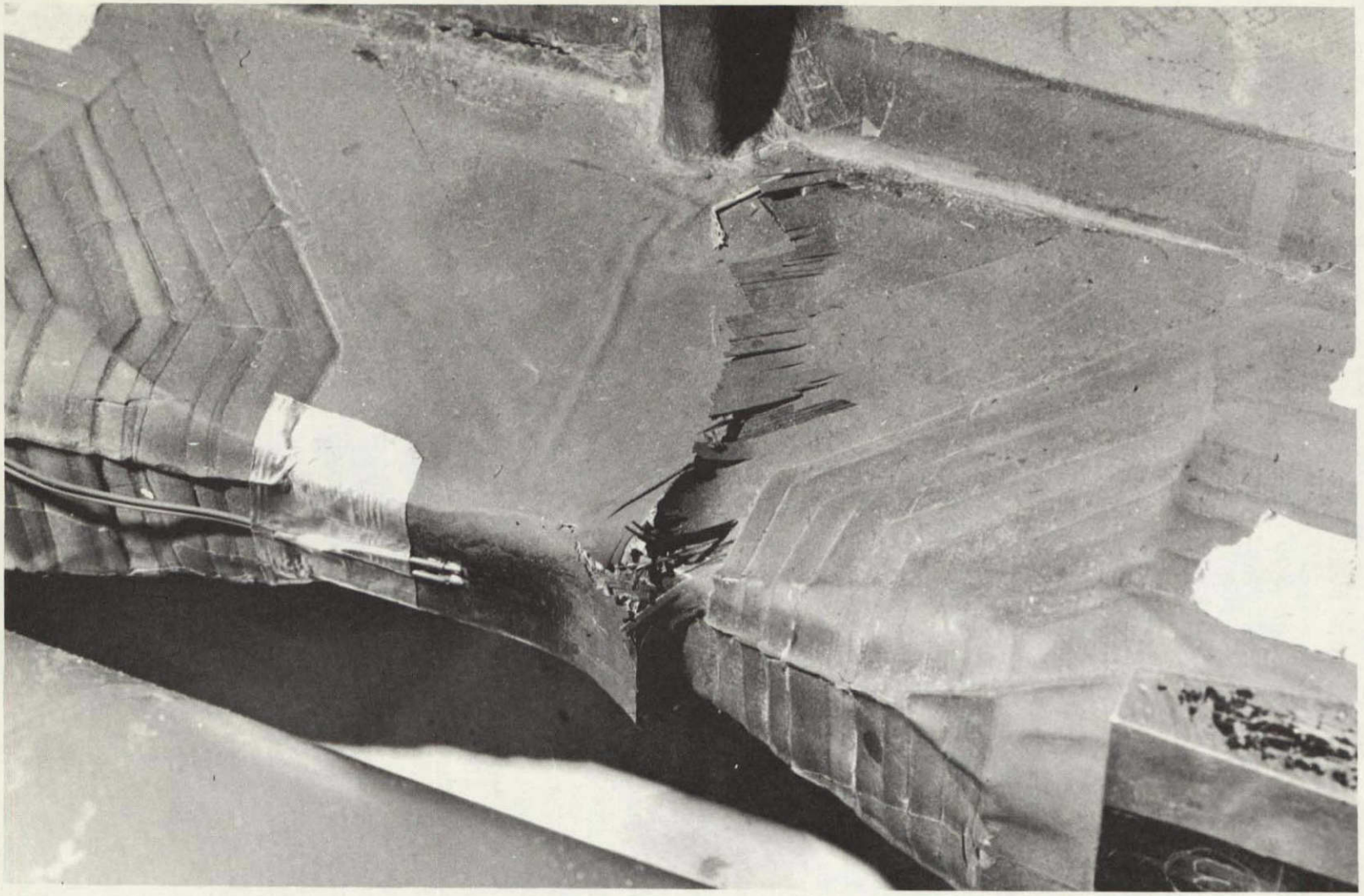

FIGURE 33. FRAME BENDING SPECIMEN #1 SHOWING FRACTURE IN UPPER CAP, EXTENDING THROUGH WEB TO LOWER CAP.

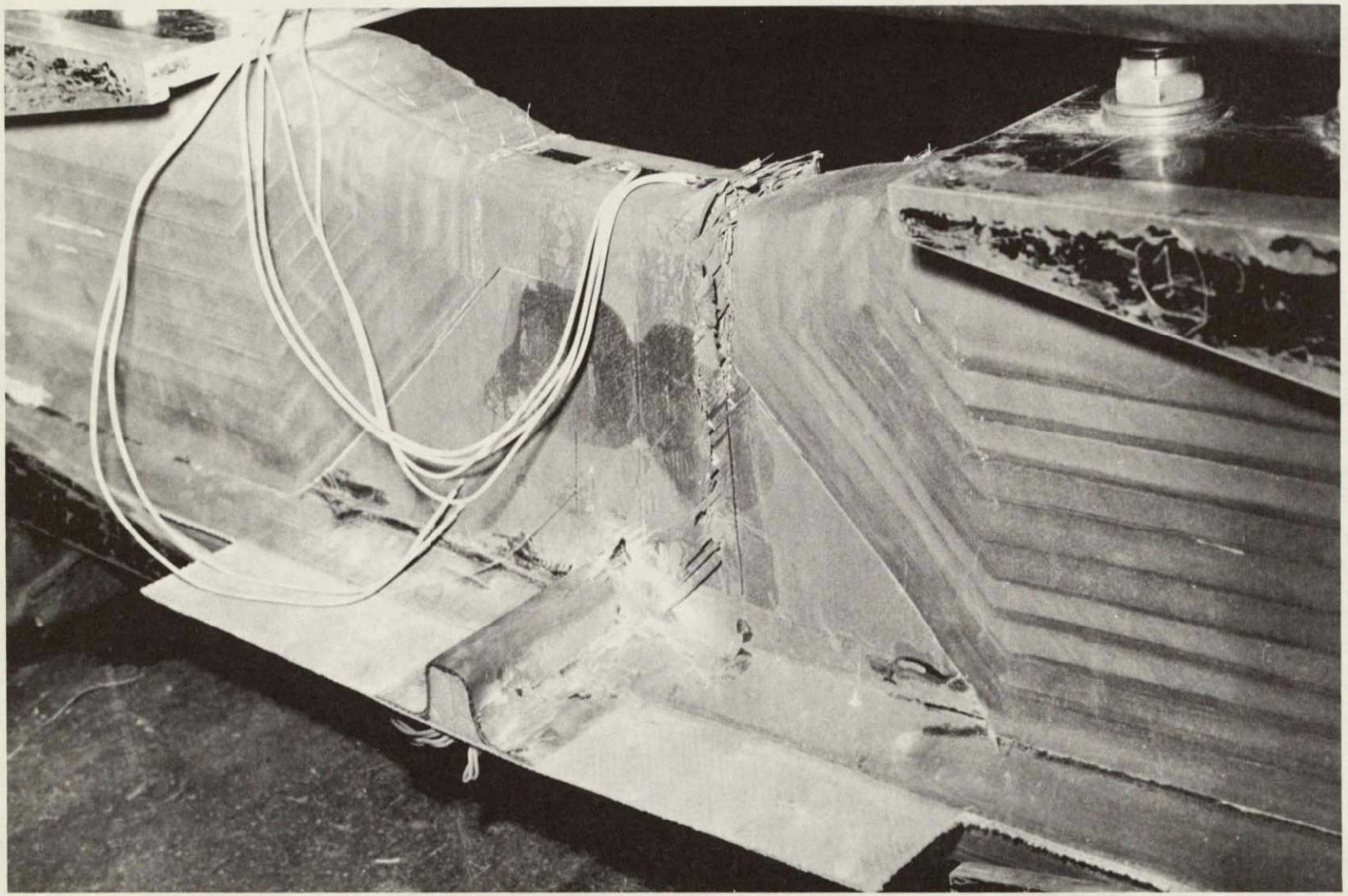

FIGURE 34. FRAME BENDING SPECIMEN #2 SHOWING FRACTURE IN UPPER CAP, EXTENDING THROUGH WEB TO LOWER CAP.

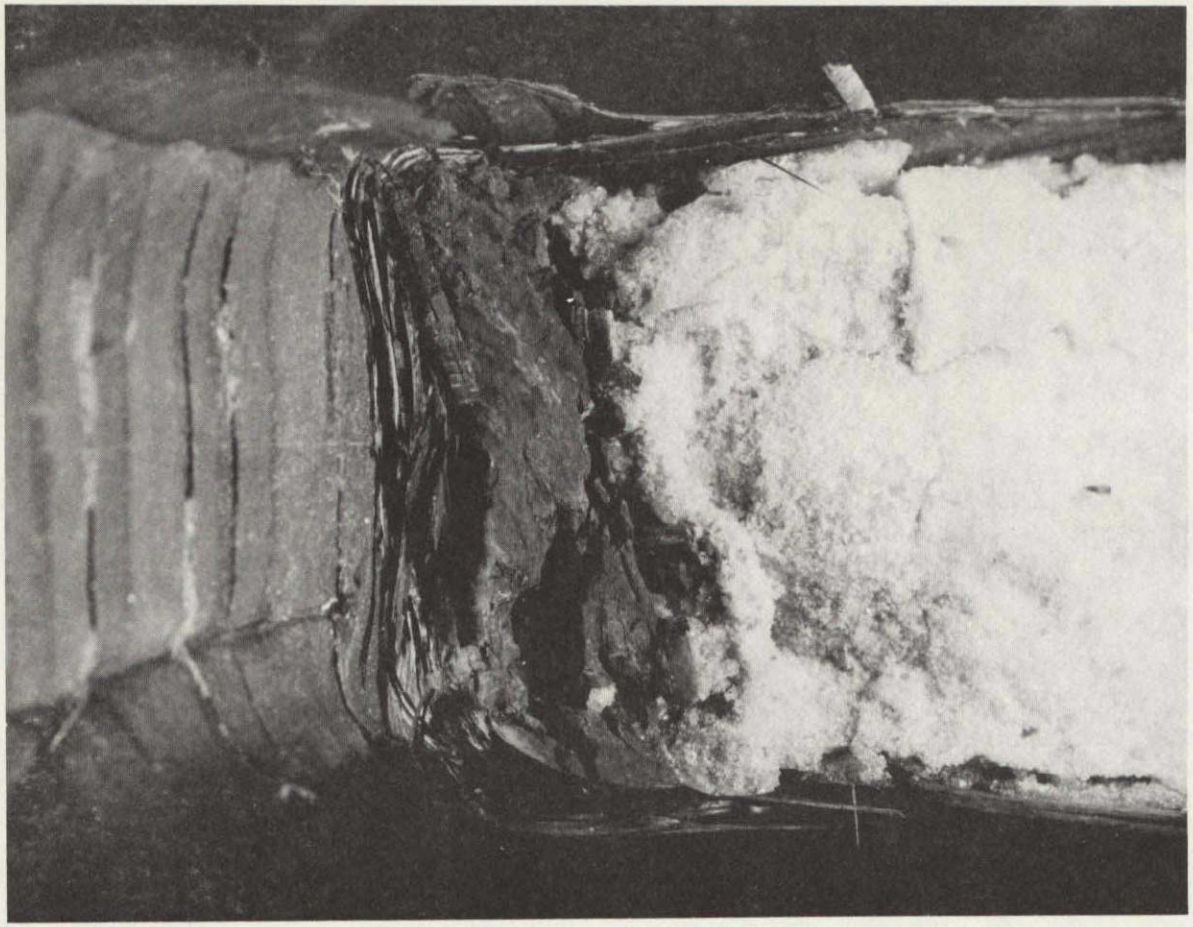

FIGURE 35. FRAME BENDING SPECIMEN #1, SECTIONED AT PLANE OF FRACTURE TO REVEAL COMPRESSION BUCKLING OF 0° GRAPHITE CAP LAMINATE.

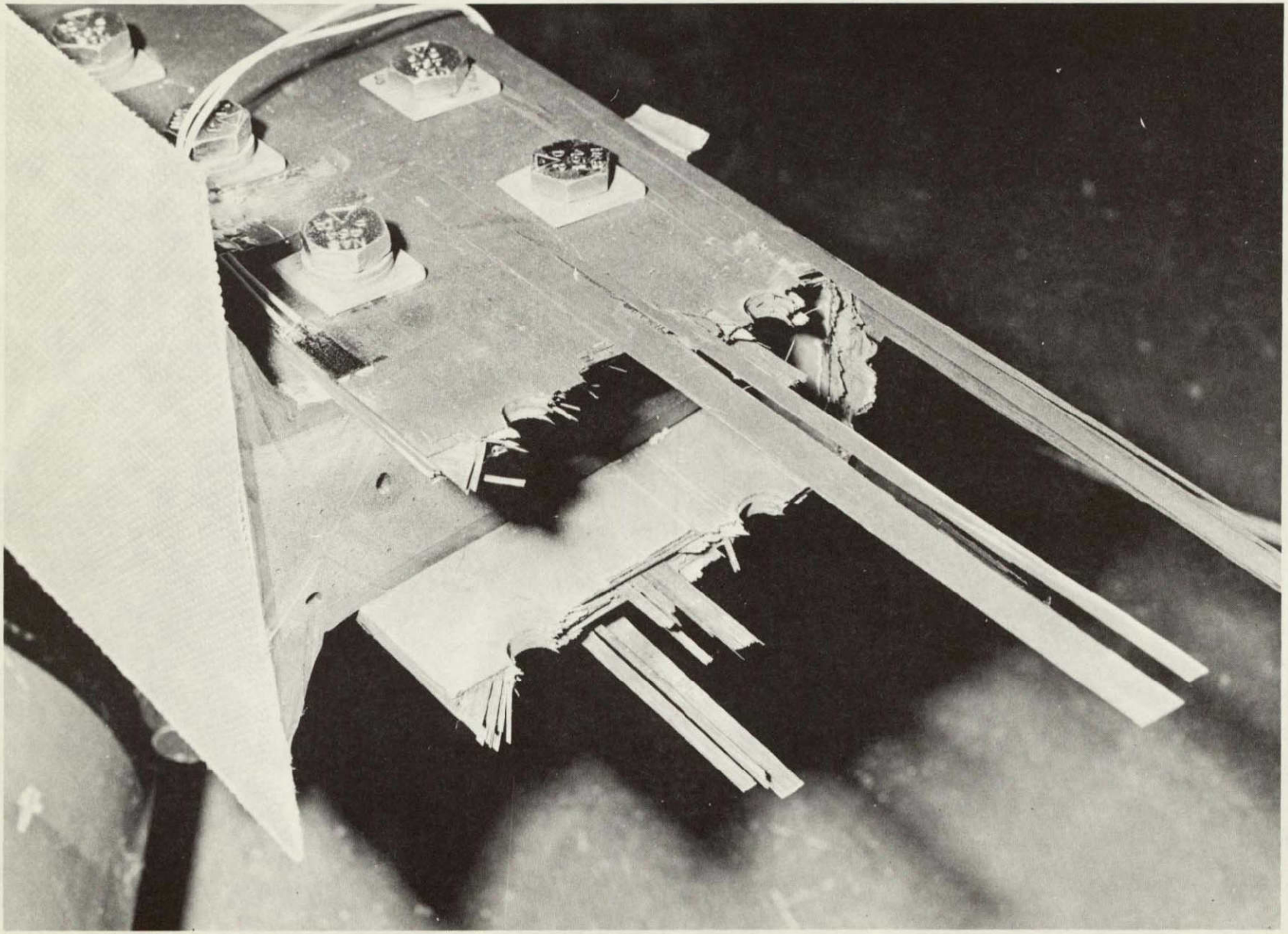

FIGURE 36. FRAME SPLICE BENDING SPECIMEN #1 SHOWING FRACTURE OF FRAME SPLICE CAP AT ATTACHMENT HOLES.

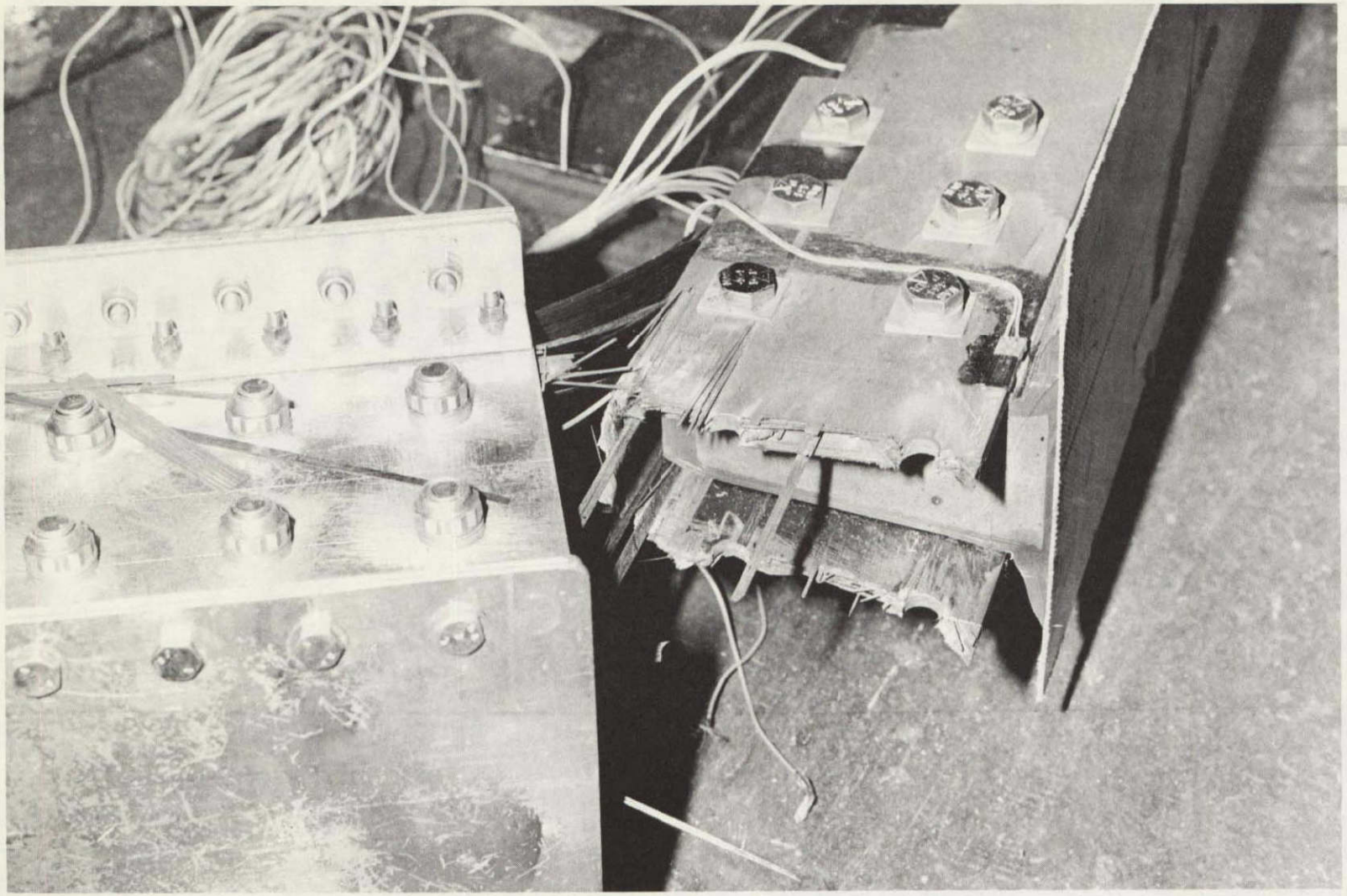

FIGURE 37. FRAME SPLICE BENDING SPECIMEN #2 SHOWING FRACTURE AT TEST FIXTURE ATTACHMENT HOLES.

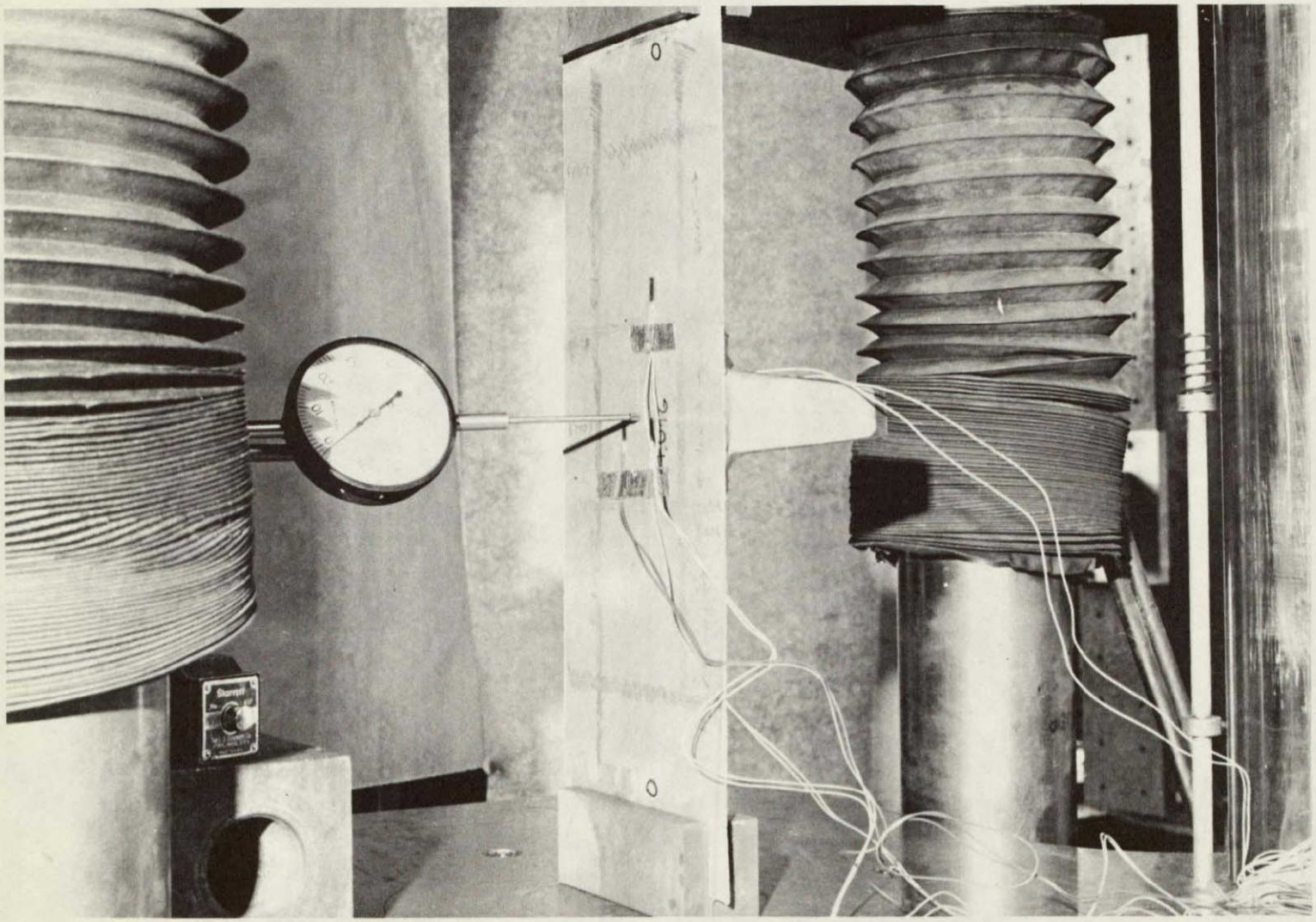

FIGURE 38. STRINGER TEST SPECIMEN IN BALDWIN UNIVERSAL STATIC TEST MACHINE

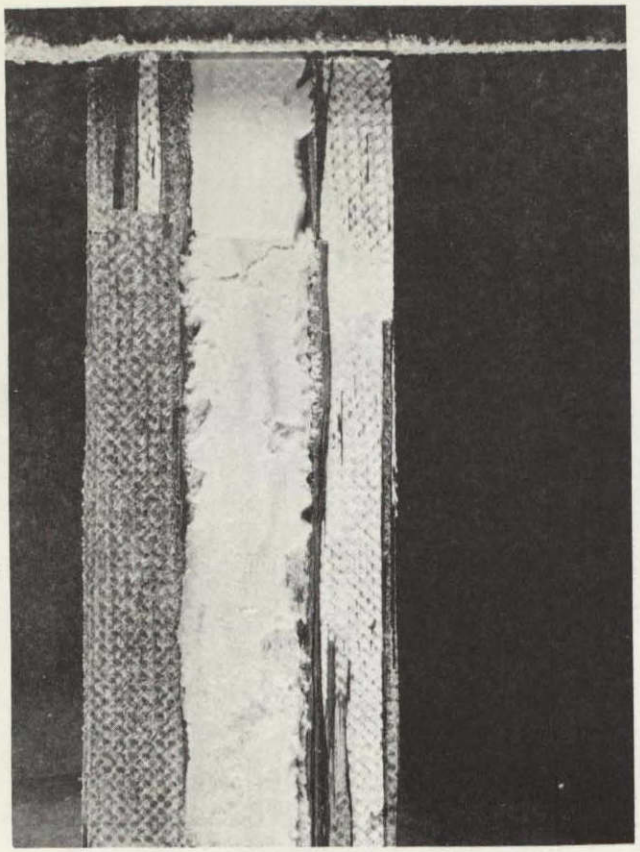

(a) SPECIMEN #1

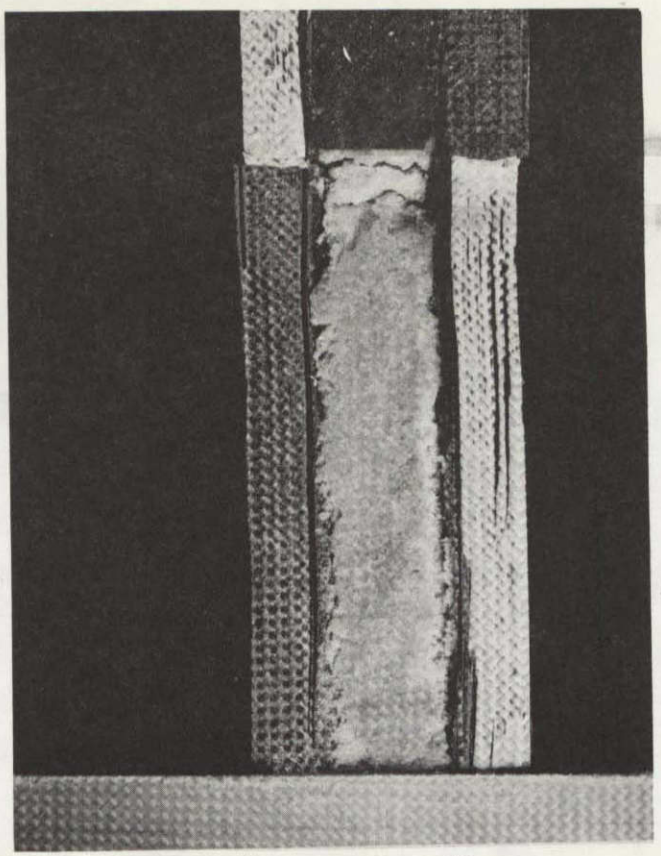

(b) SPECIMEN #2

FIGURE 39. INITIAL FAILURE OF STRINGER TEST SPECIMEN OCCURED WHEN SKIN LAMINATE SEPARATED FROM STRINGER FLANGE LAMINATE.

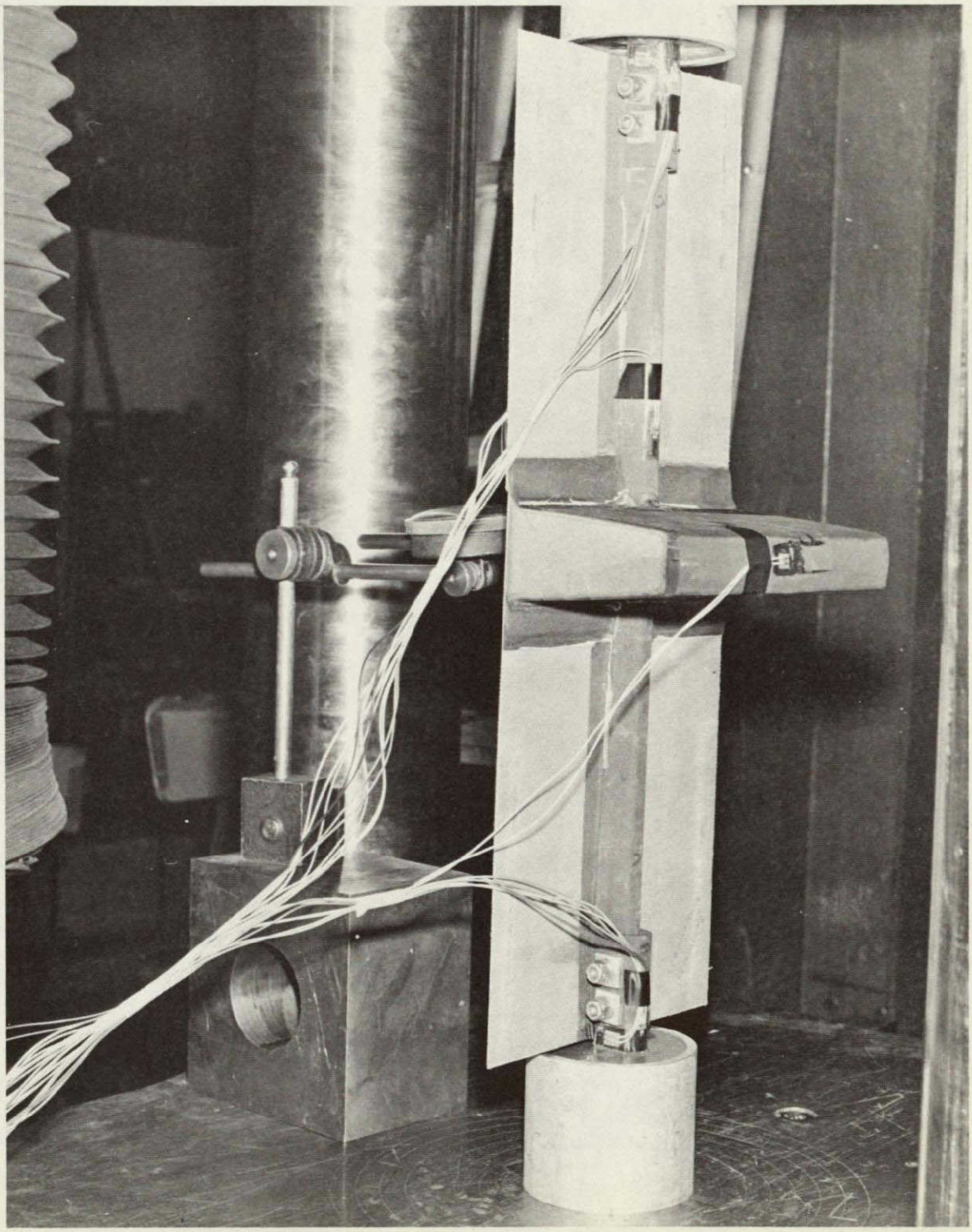

FIGURE 40. STRINGER SPLICE JOINT TEST SPECIMEN IN BALOWIN UNIVERSAL STATIC TEST MACHINE

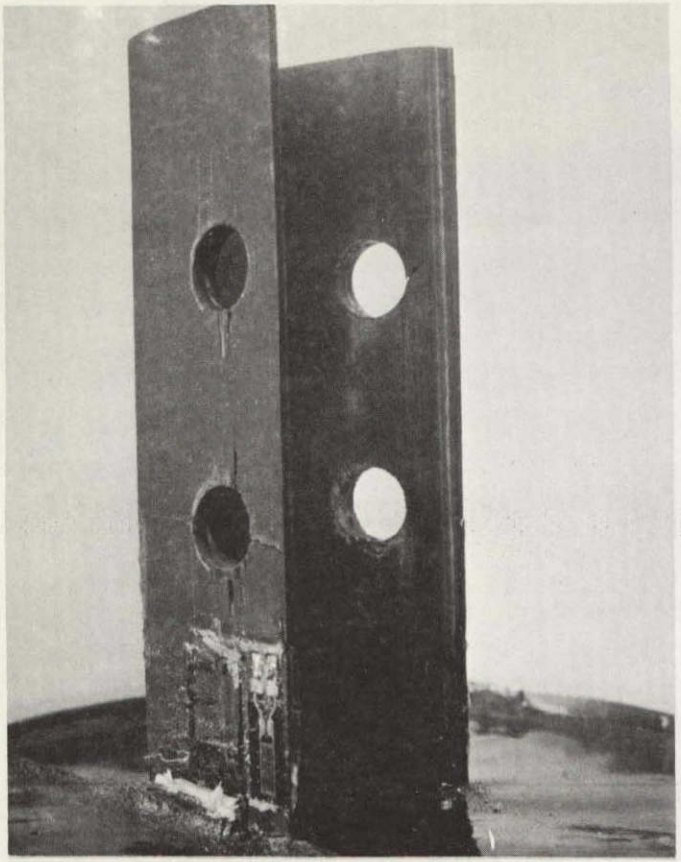

(a) SPECIMEN #1

(b) SPECIMEN #2

FIGURE 41. STRINGER SPLICE JOINT CAP FAILURES.

damage modes, the splice joint was capable of sustaining continued load at a lower level. The second specimen failed at 14.68 kN (3300 lb). The strain at fracture was 9200 μ inches/inch. Fracture of the splice cap occurred adjacent to the potting compound as shown in Figure 41b and is a complete compression fracture of the splice cap laminate as evidenced by a brooming type failure of the fibers extending from one edge of the splice cap laminate to the other.

6.3 COMPARISON OF ANALYSIS AND TEST RESULTS

The analysis of the stringers, frames and joints, as presented in Section 2, contains positive margins of safety. These margins of safety are the result of either practical solutions for number of plies, or prevention of premature damage prior to total fracture. A proper comparison of analytical predictions with test results should include these margins of safety for the specific fracture mode. The comparison shown in Table VIII indicates that predicted analytical failure loads are good to excellent except for the conservatism found for the frame splice.

TABLE VIII

COMPARISON OF ACTUAL FAILURE LOADS VS DESIGN PREDICTIONS

STRUCTURE	DESIGN ULTIMATE LOAD	PREDICTED FAILURE LOAD ZERO MARGIN OF SAFETY	TEST FAILURE LOAD (AVERAGE)	RATIO OF TEST TO PREDICTED FAILURE LOAD	RATIO OF TEST TO DESIGN LOAD	COMMENTS
STRINGER COMPRESSION	20 016 N (4500 lb) (COLUMN)	31 447N (7070 lb) (CRIPPLING)	29 579N (6650 lb)	.94	NO EQUIV. TEST	DEMONSTRATES CRIPPLING IS NOT A PROBLEM AND ADEQUATE MARGINS OF SAFETY SHOULD EXIST FOR COLUMN MODE
STRINGER SPLICE COMPRESSION	13 344N (3000 lb)	14 678 N (3300 lb)	15 123N (3400 lb)	1.03	1.13	
FRAME AXIAL AND BENDING	73 836N (16,600 lb) 11 291N·m (100,000 in.lb)	85 668N (19,260 lb) 13 505N·m (116,000 in. lb.)	67 609N (15,200 lb) 11 066N·m (98,000 in.lb)	.84	.98	WHILE TEST VERIFIES DESIGN THE ANALYTICAL PREDICTION IS SIGNIFICANTLY LOWER THAN TEST RESULTS
FRAME SPLICE AXIAL & BENDING	14 678N (3300 lb) 2 258N·m (20,000 in.lb)	23 930N (5,380 lb) 3 681N·m (32,600 in.lb.)	35 761 N (8,040 lb) 5 587 N·m (49,470 in.lb)	1.49	NO DATA FOR FIBER FAILURE MODE	COMPARISON SHOWS THAT A MORE PRECISE ANALYTICAL PROCEDURE IS NEEDED FOR COMPLEX SPLICES WHERE AXIAL & BENDING LOADS ARE INTRODUCED. IN ADDITION SOME CONSERVATISM IS PROBABLY DUE TO HOLE SIZE EFFECT.

SECTION 7.0 CONCLUSIONS

1. The static structural adequacy of the skin/stringer/frame sections, fabricated by the single cure process was demonstrated by the structural tests.

2. The single cure fabrication process as developed for the eight skin/stringer/frame specimens has been proven practical for the intended application. The process, as developed has significant potential for fabrication of larger more complex multiple frame/stringer element structures.

3. The analysis used for the design of the splice joint for the frame sections is approximate and tends to be good to excellent except for the conservative frame splice. Precise prediction of ply buildup/orientation requirements dictates the utilization of a finite element analysis, or an iterative analysis/test/analysis program utilizing the present Carnagie-Mellon analysis program.

4. Production of reproducible foam details on an economical basis requires the utilization of foam metering/dispensing equipment.

5. The shell mold tooling concept, fabricated to the outside mold line of the tool, with positioning pin/angle locators for the foam core members, was suitable for fabrication of the flat frame/stringer/skin test elements and has potential for fabrication of large multiple frame/stringer element structures.

THIS PAGE LEFT INTENTIONALLY BLANK

SECTION 8.0 REFERENCES

1. Rich, M.J.; Ridgley, G.F.,; and Lowry, D.W.: Application of Composites to Helicopter Airframe and Landing Gear Structures, NASA CR-112333, 1973.

2. Advanced Composites Design Guide. Advance Development Division, Air Force Material Lab Wright Patterson Air Force Base Ohio, Air Force Systems Command, January 1973.

3. Waszczak, John P.: A Synthesis Procedure for Mechanically Fastened Joints in Advanced Composite Materials. PHD Thesis Carnage-Mellon. University Report No. SM-73-11, 1973.

4. MIL-HDBK-5B. Military Standardization Handbook, Metallic Materials and Elements for Aerospace Vehicle Structures, September 1971.